LIST OF RESEARCH PAPERS PUBLISHED

Sr. No.	Title of paper	Name of the author/s	Department of the teacher	Name of journal	Year of publication	ISSN number
1.	Surface Conductivity of Binary Carbonate as a Performance Governing Parameter of an Electrochemical CO2 Gas Sensor	Prashant Ambekar and Jasmirkaur Randhawa	Physics	Bull. Mater. Sci. (2021) 44:235	2021	10.1007/s 12034-021-02526-y
2.	Study Of Thermal and Electrical Properties of Aluminum Cerium Alloy with Varying Cerium Doping for High Energy Storage Battery Applications	P. W. Ambekar, P. Y. Deshmukh, S. K. Ubale & S. B. Misra	Physics	AAI Journal, Vol. 21 pp 20-25• Issue No. 3	2021	ISSN: 2581-6055
3.	Ionic and Electronic Transport Studies of Na-Glass Dispersed Ag2SO4 Composite Electrolyte for Electrochemical SO2 Gas Sensor Application	Jasmirkaur Randhawa & Prashant Ambekar	Physics	VIIRJ	2021	ISSN: 2319-4979

4.	Charge transfer mechanism in KNbO3 dispersed composites of monovalent alkali carbonate. Ferroelectrics	Prashant Ambekar, Jasmirkaur Randhawa and Kamal Singh	Physics	FERROELECTRICS	2022	DOI: 10.1080/00150193.2022.2034418
5.	Investigation of the Role of Goal Setting Objectives and its Outcomes among Young Learners	Dr.Shraddha Deshpande	English	International Journal of English Literature and Social Sciences	2021	ISSN: 2456-7620 DOI:10.22161/ijels.64.1
6.	SWOT Analysis of Clean Fuel Programme Initiative In India	Dr.Vaishali Jaiswal, Dr Vaishali Meshram and Dr. Pravin Meshram	Chemistry	International Journal of Researches in Biosciences, Agriculture and Technology	2022	e-ISSN 2347 - 517X 2.2394-7780
7.	PREPARATION AND STRCUTURAL STUDIES OF SOME BIS POLYMERIC COMPLEXES	Dr. Vaishali Meshram	Chemistry		2021	

Prof. Pitambar Humane
IQAC Co-ordinator

CO ORDINATOR
INTERNAL QUALITY ASSURANCE CELL
DHARAMPETH, M. P. DEO MEMORIAL &
SCIENCE COLLEGE, NAGPUR

Dr. Akhilesh Peshwe
Principal

Principal
Dharampeth M.P. Deo Memorial
Science College, Nagpur.

Bull. Mater. Sci. (2021)44:235
https://doi.org/10.1007/s12034-021-02526-y

Surface conductivity of binary carbonate as a performance-governing parameter of an electrochemical CO_2 gas sensor

PRASHANT AMBEKAR[1,*] and JASMIRKAUR RANDHAWA[2]
[1]Dharampeth M. P. Deo Memorial Science College, Nagpur 440033, India
[2]Government College of Engineering Nagpur, New Khapri, Nagpur 441108, India
*Author for correspondence (pacific0701@gmail.com)

MS received 2 February 2021; accepted 27 June 2021

Abstract. In electrochemical CO_2 gas sensor, the chemical potential of electrolyte changes on adsorption of CO_2 molecules as the process involves catalytic electron transfer. In addition, it is the rate-determining step that decides sensor's response. In this study, *in-situ* bulk AC, DC and surface electronic conductivities of $CaCO_3 + Li_2CO_3$ binary solid electrolyte were investigated at different temperatures and CO_2 gas partial pressures using complex impedance spectroscopy, Wagner's DC polarization technique and four-probe method, respectively. For the four-probe conductivity measurements with crucial requirement of high temperatures and test gas variations, a customized sample holder was designed and fabricated having gold-plated equidistant, spring-loaded electrodes and localized heating system (maximum 593 K). The AC bulk conductivity was found to decrease with rise in CO_2 gas concentration (from 0.1 to 100%) by about two orders and one order of magnitudes at lower and higher temperatures, respectively. Similarly, surface conductivity variation with temperature also showed Arrhenius behaviour for both the concentrations of CO_2 viz. 0.04 and 10%, giving lower value of activation enthalpy for lower CO_2 concentration. The surface conductivity change in the presence of different concentrations of CO_2 gas is justified by comparing with AC bulk conductivity measurements at different CO_2 partial pressures and DC conductivity along with sensing response. The mechanism is explained using activated charge transfer data. The range of E_a values on adsorption of CO_2 gas was found to be in the electronic excitation window, suggesting involvement of a new parameter to be investigated for non-Nernstian response of EC sensors.

Keywords. Charge transfer reaction; electrochemical CO_2 gas sensor; complex impedance spectroscopy; solid electrolyte; surface conductivity.

1. Introduction

Solid electrolyte is an important component of electrochemical gas sensor, which enables ions' transport through it under the electrochemical potential gradient between the opposite surfaces viz. test and reference electrodes. Ideally, this component is an ionic conductor with negligibly small electronic conductivity [1]. While sensing, on the adsorption of gas under test, its surface electronic conductivity may change as the process of gas adsorption involves catalytic electron transfer. This could be one of the rate-determining processes deciding the response time of sensor [2].

Gas sensors used in industry and in pollution monitoring systems should be reliable in terms of reproducibility, reversibility, fast response time, wide gas detection range, negligible cross-sensitivity, long-term operation, resistant to thermal shocks and follow theoretical laws such as Nernst's principle in case of electrochemical sensor. For electrochemical sensor fabrication, multi-component electrolyte systems are attractive owing to their better chemical stability and inherent high ionic conductivity compared to those of mono-component electrolyte [3]. The potentiometric CO_2 gas sensors based on mono-component electrolyte have been required to be operated at high temperature (~973 K) [4–6]. Also, highly hygroscopic nature of pure alkali carbonate Li_2CO_3, K_2CO_3, Na_2CO_3, etc. has restricted its use, as an electrolyte, in electrochemical detection of CO_2 gas under humid condition, since it drifts the cell's electromotive force (EMF) with time [7]. Addition of divalent carbonates to the pure mono-valent alkali carbonate, e.g., Li_2CO_3, enhances ionic conductivity and reduces cross-sensitivity to moisture [8]. Moreover, they provide good interface with reference electrode materials, which are generally tertiary oxides of alkali earth metals [6].

Potentiometric sensors developed using binary electrolytes have been found working better in terms of response time and sensitivity [2]. On comparing the characteristics of CO_2 sensors with different electrolytes, it has been observed that response time is strongly dependent on electrolyte's surface [2]. The variation of electrolyte

Published online: 26 August 2021

properties on adsorption of gases viz. surface conductivity (electronic/ionic) is thought to be one of the probable reasons. The *in-situ* surface conductivity of the electrolyte material cannot be measured while sensor is in operation due to interference of reference and test electrode potentials. So far, no attempt has been made in studying the surface conductivity of solid electrolyte or to be precise the gas-sensing surface of an electrochemical sensor. Therefore, in this study, the *in-situ* bulk AC and DC conductivities of $CaCO_3$ + Li_2CO_3 binary solid electrolytes were investigated at different temperatures and CO_2 gas partial pressures using complex impedance spectroscopy and Wagner's DC polarization technique, respectively. In addition, the surface electronic/ionic conductivity measurements with the presence and absence of CO_2 gas in embedded air were conducted by using four-probe method [9].

2. Experimental

2.1 *Materials preparation and structural characterization*

For preparation of binary electrolyte, well dried carbonates Li_2CO_3 and $CaCO_3$ from Merck with purity 98 and 98.5%, respectively, were taken in appropriate weight fractions to produce a mixture for two binary series viz. $(100–x)Li_2CO_3 + x(CaCO_3)$. The carbonates were mixed thoroughly under acetone (AR grade) and then temperature was raised slowly to the melting point, i.e., 996 K. After soaking for half an hour at the same temperature, the molten mixture was quenched rapidly to room temperature between clean aluminium plates, resulting into flakes of thickness roughly about 1–2 mm. The so-obtained flakes with uniform thickness and diameter ($\sim$10–12mm) were used for further study of surface conductivity measurement. Electrodes were formed on the surface by four equidistance dots of Ag paint of size $\sim$1 mm diameter. The structural characterization was done by powder XRD (Bruker D8 XRD unit, Cu 1.54 AU) with 2θ values ranging from 5 to 80°.

2.2 *Electrical characterization*

2.2a *Impedance Analysis:* AC electrical conductivity of the electrolyte was measured using complex impedance spectroscopy in the frequency range 5 Hz to 13 MHz (HP4192A impedance analyzer) at different temperatures (473–773 K). Samples were taken in the form of circular pellets obtained by taking polycrystalline binary carbonate powder with crystallite size <40 micron compressed uniaxially using hydraulic press at a pressure of 3 ton cm^{-2}. The pellets were sintered at temperature 873 K for 8 h to obtain maximum density and then sputtered with gold for electrode formation. The value of bulk resistance was measured at the X-axis intercept of the trace, at which the imaginary part is zero. The analysis was done manually using MS-Excel. The ionic nature of the binary electrolyte was confirmed by Wagner's DC polarization technique. The similar sample pellet as used in impedance measurement with inert electrodes was subjected to fixed DC potential (500 mV) and the current was noted as a function of time. The ionic and electronic transference number (t_i and t_e) were estimated from the zero time and infinite time conductivities, respectively.

2.2b *In-situ surface conductivity:* For the four-probe assembly with crucial requirement of high temperature and gas-embedded measurements, an indigenous sample holder was designed and fabricated (figure 1). Four-probe assembly with gold-plated equidistance spring-loaded electrodes and testing temperature range from RT to 593 K was fabricated. This unit has localized heating system, which reduces power consumption with fast equilibrium. The assembly is encapsulated in a glass jar, which enables to perform measurements in atmosphere of choice. The gases either ambient air or calibrated were passed through a water column of 5 cm in order to achieve similar humidity conditions in different cases. The sample holder assembly is also assisted with a digital PID temperature controller and gas flow facility. The system can be utilized for different electrical measurements such as two-probe/four-probe DC and AC measurements.

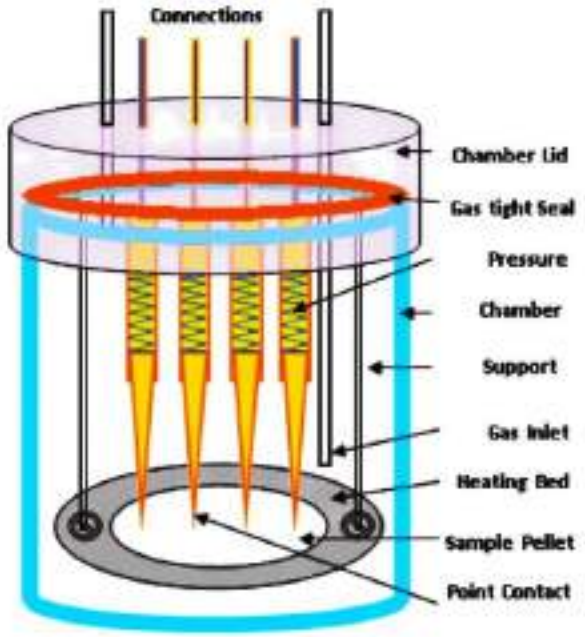

Figure 1. Four-probe assembly developed indigenously for measurement of *in-situ* surface conductivity of electrolyte.

3. Results and discussion

3.1 *Structural analysis*

The powder X-ray diffraction analysis for the binary compositions $70Li_2CO_3 + 30CaCO_3$ showed that all major peaks identified in the diffraction patterns matched with $CaCO_3$ and Li_2CO_3 (JCPDS data file no. 85-0849 and 83-1454) with no extra identifiable peak. This confirmed the formation of a bi-phase mixture without any solubility (figure 2). The values of crystal size and lattice strain have been determined using Scherrer's formula [10]. In the $70Li_2CO_3 + 30CaCO_3$ system, the average values of crystallite size for $CaCO_3$ and Li_2CO_3 are found to be 46.85 and 47.65 nm, respectively, and the values of lattice strains are found to be 0.00245 and 0.0027, respectively, which are found comparable in both the crystallites.

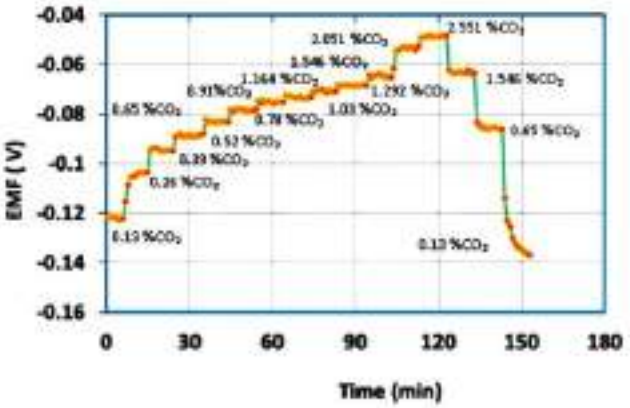

Figure 3. Typical electrochemical sensor response for CO_2 partial pressure in air from 0.13 to 2.551% at 673 K.

3.2 *Sensor performance study*

Response of an electrochemical CO_2 gas sensor with $Li_2CO_3 + CaCO_3$ electrolyte cum test electrode having cell configuration:

$$CO_2, O_2, Au/7LC + 3CC/\text{compatible open reference electrode}/Au, O_2$$

tested under different CO_2 gas partial pressures ranging from 0.13 to 2.55% embedded in artificial air is shown in figure 3. The electrode reactions and corresponding expression for cell EMF, E, are expressed as:

$$\text{At test electrode: } Li_2CO_3 \Leftrightarrow 2Li^+ + 2e^- + \frac{1}{2}O_2 + CO_2$$

$$\text{At reference: } MO_x + 2Li^+ + 2e^- + \frac{1}{2}O_2 \Leftrightarrow Li_2MO_{x+1}$$

$$\text{Overall reaction: } Li_2MO_3 + CO_2 \Leftrightarrow Li_2CO_3 + MO_2$$

Nernst's equation for cell EMF:

$$E = -\frac{G^oLi_2TiO_3 - G^oLi_2CO_3 - G^oTiO_2}{nF} - \frac{RT}{nF}\ln\frac{P_{CO_2}}{P^o} \quad (1)$$

In electrochemical potentiometric sensors, an open reference electrode for fixing the activity of alkali ion, a bi-phase mixture of compounds of alkali metals with transition metal oxides and transition metal oxides (in this case, Li_2TiO_3 and TiO_2) are used as per Gibb's phase rule. The empirical values of cell EMFs as per the Nernst's relation are directly calculated using Gibb's free energy values at different temperatures, which are taken from the standard thermodynamical data of pure substances [11]. The t_{90} response time was found to be <1 min. The number of electrons transferred in the cell reaction obtained from the slope (figure 4) was found to be $n = 2.52$, showing deviation from its theoretical value 2, indicating non-Nernstian behaviour of the sensor. The commercial CO_2 gas sensors developed so far are based on conventional sensing principles like optical absorption (NDIR) [12], electrical resistance [13], field-effect transistors [14] and amperometric type [15]; which have limitations as they are bulky, expensive and/or less durable [16]. A comparison of performance parameters of this sensor with that of the commercially available CO_2 sensors is given in table 1.

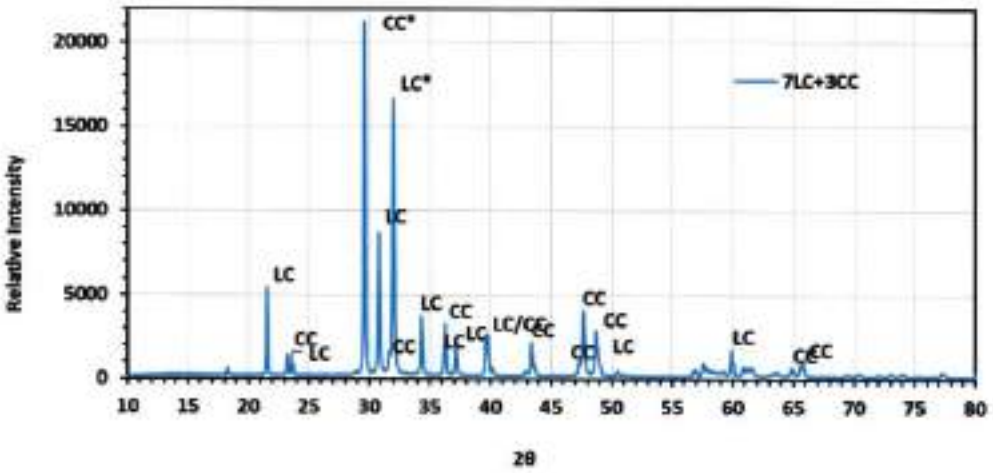

Figure 2. Powder XRD pattern of $70\,Li_2CO_3 + 30\,CaCO_3$ binary carbonate confirming bi-phase mixture.

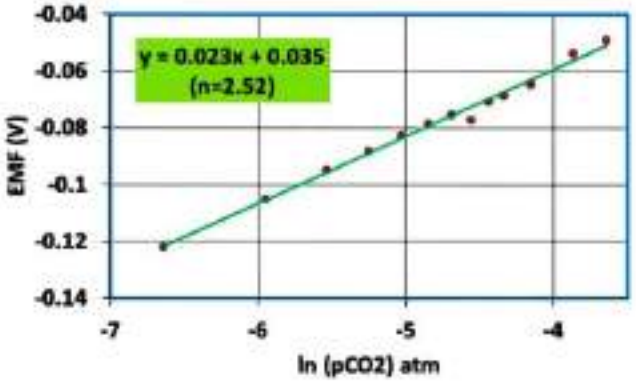

Figure 4. Plot of sensor EMF with CO_2 partial pressure showing Nernstian-type behaviour with 2.52 electron reaction.

3.3 *DC conductivity measurements*

A comparison of bulk ionic and electronic conductivities of the $70Li_2CO_3 + 30CaCO_3$ binary electrolyte is shown in figure 5, wherein sharp rise in ionic and moderate rise in electronic conduction is observed above 523K. With rise in temperature, ionic conductivity increases and saturates at the rise of about one order of magnitude ($\sigma_i = 2.6 \times 10^{-5}$ S cm^{-1}). The electronic conductivity was also found to have increased at high temperature by very small amount ($\sigma_e = 1.4 \times 10^{-6}$ S cm^{-1}), giving average ionic transference number 0.950, which signifies majorly ionic nature of the electrolyte with significant dominance of electronic conductivity. As expected from previous investigations, the electronic conduction rises with increase in ionic conduction [17].

3.4 *Complex impedance analysis*

Two depressed semicircles have been seen in the impedance plot (figure 6), which suggest two different conduction mechanisms viz. migration of cations parallel to the interface and through the bulk of the electrolyte grain, and ion migration perpendicular to the interface [18]. Values of capacitance at low and high frequency semicircles are found to be in nF and pF range. The impedance plots show the dependence of ac conductivity on CO_2 gas partial pressure at 573 K. The value of bulk resistance is seen increasing with rise in CO_2 concentration. This lowering of ionic conductivity indicates that the atmospheric CO_2 gas molecules adsorbed on the surface of electrolyte hold back the cations at the surface as per the reaction: $CO_3^{2-} + 2Li^+ \rightarrow Li_2CO_3$. Impedance spectroscopy gives bulk characteristics of the electrolyte, but here adsorbed CO_3^{2-} molecules are found responsible for decrease in the bulk conductivity, indicating that the number of charges migrating perpendicular to the surfaces is decreased as the CO_3^{2-} molecules blocks the cation. Normally in metal oxide gas sensors, if the oxide material is heated to high temperature, oxygen will adsorb on the surface and grain boundaries. However, here the maximum lowering down of the conductivity is observed for 100% CO_2 gas atmosphere. Nevertheless, the mixed effect due to oxygen and CO_2 can never be denied as the oxidation of stable CO_2 through catalytic activity for temperatures >523 K to produce CO_3^{2-} ion utilizes the oxygen from ambient air, as follows:

$$CO_2 + \frac{1}{2}O_2 + 2e \rightarrow CO_3^{2-}.$$

The Arrhenius plots for bulk AC conductivity are obtained as shown in figure 7, suggesting that the effect of CO_2 gas concentration on conductivity is significant at lower

Table 1. Comparison of commercially available CO_2 gas sensors.

Company name	Product type	Detection range (ppm)	Response/ recovery time	Operating temperature	Reference
Cubic	NDIR	0–200	30/50	Room temperature	[20]
Vaisala	NDIR	0–2000	60 /7 min	Room temperature	[21]
+MG811 air carbon dioxide (CO_2) sensor module	Metal oxide sensor	0–10000	—	Localized heating	[22]
NASA, Glenn Research Centre, OH	Electrochemical, $Na_3Zr_2Si_2PO_{12}$ electrolyte, sensing electrode $Na_2CO_3/BaCO_3$ with SnO_2 sol–gel	0.5–4%	<30 s	648 K	[23]
Present work	Electrochemical, $70Li_2CO_3 + 30CaCO_3$ electrolyte cum sensing electrode, $Li_2TiO_3 + TiO_2$ reference electrode	0.13–2.55%	<60 s	573–723 K	—

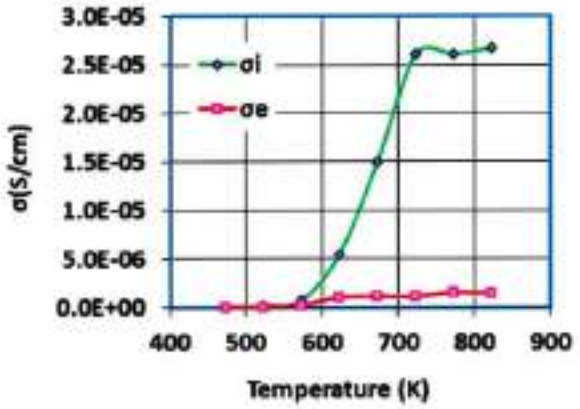

Figure 5. Variation of ionic and electronic conductivities at different temperatures measured by Wagner's DC polarization.

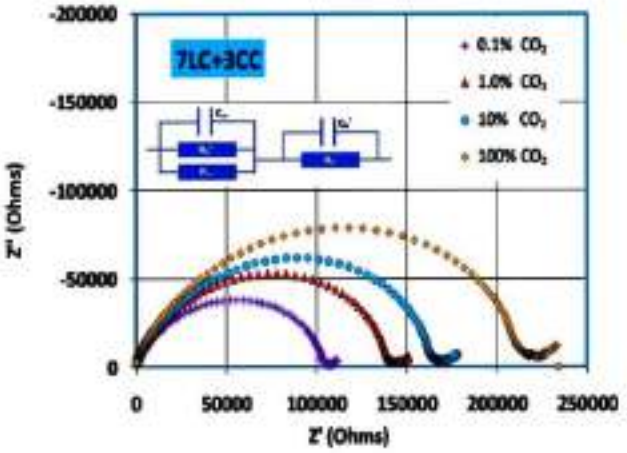

Figure 6. Impedance plots showing decrease in bulk conductivity with CO_2 concentration at 573 K is shown with equivalent circuit. Typical values of circuit parameters for 100% CO_2 gas concentration curve are: $R_b^{\perp}$ = 215 kΩ, $C_b^{\perp}$ = 0.0148 nF and $R_b^{\parallel} \| R_{\infty}$ = 81 kΩ, C_{∞} = 7.82 pF at low and high frequency values 50.118 and 251.188 kHz, respectively.

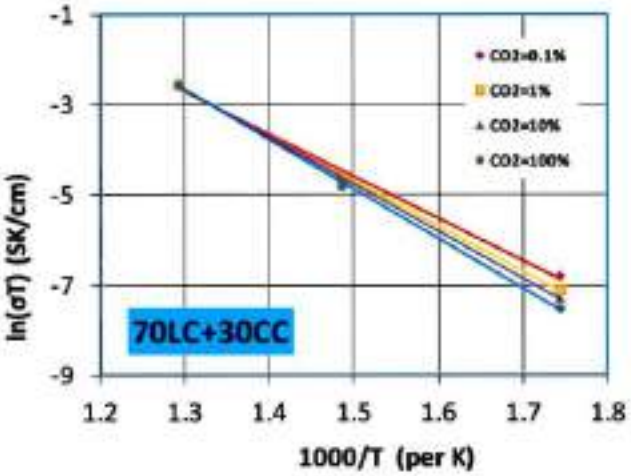

Figure 7. Arrhenius plots for 70LC + 30CC binary electrolyte system at different CO_2 partial pressures.

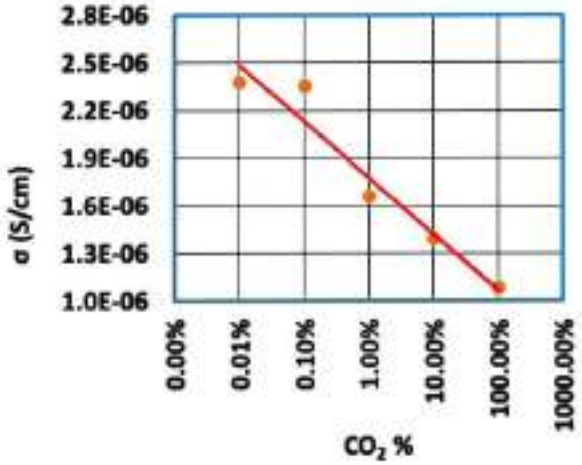

Figure 8. Logarithmic decrease in AC conductivity with CO_2 concentration at 573 K.

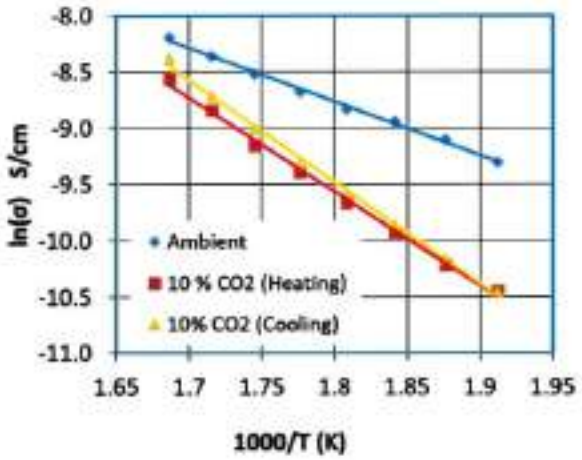

Figure 9. Variation of surface conductivity of 70LC + 30CC binary carbonate system for ambient (0.04%) and 10% CO_2 concentrations in the temperature range 513–593 K.

temperature. The AC conductivity changes by about 3 orders of magnitude over the temperature range 573–773 K. The variation in activation energies obtained from the Arrhenius plot is seen lying in the range from 0.768 to 0.902 eV. Capacitance values and activation enthalpy values together signify the mechanisms that are characteristics of ion migration through lattice defects [19]. With logarithmic increase in CO_2 concentration, the ionic conductivity is seen decreasing at elevated temperatures (573–773 K) for binary electrolyte, the decrease is within one order of change (figure 8). This lowering of ionic conductivity indicates that the atmospheric CO_2 gas molecules equilibrate with cations present on the surface of electrolyte holding it back at the surface.

3.5 *Surface electronic conductivity measurements*

The surface conductivity measurements were taken using indigenously developed four-probe unit in the temperature

range from 500 to 620 K, varying in the step of 10 K at two CO_2 gas partial pressures viz. 0.04 and 10% embedded in artificial air. Variation of surface conductivity with temperature for $70Li_2CO_3 + 30CaCO_3$ system for two CO_2 gas concentrations is shown in figure 9. The plots for 10% CO_2 in embedded air for heating and cooling cycles are seen overlapped confirming the reproducibility of measurements at different temperatures. It also signifies that the temperature equilibrium attended by the sample/sample holder is quick and trust worthy. The plot for open atmosphere (ambient) shows change in conductivity with temperature linearly but with lower value of activation energy. However, the plots for 10% CO_2 partial pressure shows relatively larger activation energy, and conductivity found shifted almost more than two orders and one order at lower and higher temperatures, respectively. For the $70Li_2CO_3 + 30CaCO_3$ binary, the activation energy E_a is seen shifted from 2.01 to 3.94 eV, after exposure of 10% CO_2 molecules in embedded air, which signifies the adsorption process thereby changing surface electronic conductivity. Significant variation in the E_a values confirms the role of ionic configuration of the electrolyte in deciding the surface electronic conductivity. The values of E_a are found almost doubled with increase in CO_2 gas partial pressure from ambient (0.04%) to 10%, confirming the change in chemical potential of Li^+ ion with increase in CO_2 gas concentration as expected. This rise suggests more bound state of electronic (holes/electrons) charges, indicating adsorbed gas molecules bind the surface ions (Li^+), which intern resists the liberation of electrons (adsorption process of CO_3^{2-}). This is apparently seen as an order of magnitude fall in surface conductivity values with increase in CO_2 partial pressure. The values of activation energy lying in the visible region of electromagnetic spectrum suggest the electron–donor–acceptor complex commonly seen in most charge transfer complexes in inorganic chemistry, such as Warburg element.

4. Conclusion

Bulk ionic and surface DC conductivities of binary carbonate $70Li_2CO_3 + 30CaCO_3$ deceases with increase in CO_2 gas concentration at elevated temperatures. Complex impedance analysis and comparison of activation energy values suggest that change in chemical potential and surface electronic conductivity is due to the adsorption of CO_3^{2-} ions. The surface electronic conductivity measurements at different CO_2 gas concentrations infer dominance of electronic conductivity in governing the performance of EC gas sensors. This type of investigation is carried out for the first time and it opens-up a new parametric study to probe non-Nernstian behaviour commonly observed in electrochemical gas sensor.

Acknowledgement

UGC Western Regional Office, Pune, is greatly acknowledged for financial support in carry out this work.

References

[1] Chandra S 1981 *Super ionic solids: principles and applications* (Amsterdam, North-Holland: Elsevier Science Ltd.) ISBN-13: 978-0444860392
[2] Ambekar P, Randhawa J and Singh K 2014 *Adv. Sci. Lett.* **20** 565
[3] Janata J and Huber R J (eds) 1985 *Solid state chemical sensors* (Orlando: Academic Press Inc.) ISBN: 0-12-380210-5
[4] Dietz J H 1982 *Solid State Ion* **6** 175
[5] Josowicz M and Janata J 1988 *Solid State Ion* **28** 1625
[6] Weppner W 1986 *Proc. 2nd Int. meeting on chemical sensors* Bordeaux, France p 59
[7] Singh K, Ambekar P and Bhoga S S 2002 in *Solid state ionics: trends in new millennium* B V R Chowdhari *et al* (eds) (Singapore: World Scientific Publishing Co.) p 469
[8] Haynes W M 2010-11 in *CRC handbook of chemistry and physics* David R Lide and William M Haynes (eds) (Taylor & Francis) p 91
[9] Smits F M 1958 *Bell Syst. Tech. J.* **37** 711
[10] Scherrer P 1918 *Gottinger Nachrichten Gecell.* **2** 98
[11] Barin I 1993 *Thermochemical data of pure substances* 2nd edn (Weinheim: VCH) vol 1 and 2
[12] Starecki F, Charpentier F, Doualan J-L, Quetel L, Michel K, Chahal R *et al* 2015 *Sensor Actuat. B Chem.* **207** 518
[13] Xiong Y, Xue Q, Ling C, Lu W, Ding D, Zhu L *et al* 2017 *Sensor Actuat. B Chem.* **241** 725
[14] Ersöz B, Schmitt K and Wöllenstein J 2020 *Sensor Actuat. B Chem.* **317** 128201
[15] Huang X J, Aldous L, O'Mahony A M, Campo F J D and Compton R G 2010 *Anal. Chem.* **82** 5238
[16] Rezk M Y, Sharma J and Gartia M R 2020 *Nanomaterials* **10** 2251
[17] Nafe H, R Waser, S Hoffmann, D Bonnenberg and Ch. Hoffmann (eds) 1994 *Electroceramics IV* (Germany: University of Technology) (vol II) p 745
[18] Randhawa J B, Ambekar P, Singh K and Bhoga S S 2004 *Ionics* **10** 45
[19] Hariharan K and Maier J 1995 *J. Electrochem. Soc.* **142** 3469
[20] https://en.gassensor.com.cn/index.html
[21] https://www.vaisala.com/sites/default/files/documents/GMW80-Series-Datasheet-B211435EN.pdf
[22] https://www.electronicscomp.com/gas-sensor/mg811-air-carbon-dioxide-co2-sensor-module
[23] Hunter G W and Xu J C 2008 US Patent nos. 8,702,962 and 8,052,854, https://technology.nasa.gov/patent/LEW-TOPS-59

TECHNICAL PAPER

STUDY OF THERMAL AND ELECTRICAL PROPERTIES OF ALUMINIUM CERIUM ALLOY WITH VARYING CERIUM DOPING FOR HIGH ENERGY STORAGE BATTERY APPLICATIONS

P. W. AMBEKAR[1], P. Y. DESHMUKH[2], S. K. UBALE[1], S. B. MISRA[2]
[1]Dharampeth M. P. Deo Memorial Science College, Nagpur-
[2]Minex Metallurgical Co. Ltd., 301 Rajguru Apartments, 3 New Nagardas Road, Andheri East, Mumbai
Corresponding Author: Pallavi Deshmukh {pallavi.deshmukh@minexindia.com}

Abstract
The Aluminium- Cerium (AlCe) alloys with Cerium content from 1-8 % in Al were cast in the sand-casting mould by adding Ce% into EC grade Al (99.97% purity). The thermal conductivity, electrical conductivity and metallography analysis were measured for each alloy. The microstructural and elemental analysis was done by JEOL Scanning Electron Microscope (SEM) with Brooker EDS. The electrical and thermal conductivities were found to be in the increasing order with decreasing Ce%, from 8 % to 1% gradually. The microstructure shows the fine grains formation of average size of 77 µm for AlCe1% alloy. A correlation was observed between the electrical, thermal and mechanical properties for all prepared compositions of AlCe alloy. The results indicate that AlCe alloys with lower Ce content (1-2%) makes a more superior structure of Al grains and have higher electrical and thermal conductivity properties especially with lower Cerium content.

Keywords — AlCe alloy, Electrical Conductivity, Grain Size, Microstructure Characterisation, Thermal Conductivity

1. INTRODUCTION

Thermal conductivity of materials is measured for its ability to pass a known amount of heat through it. The effectivity of transfer of heat through surroundings depends on the thermal conductivity of the materials. The materials with poor thermal conductivity resist heat flow and also obtain heat slowly from their surroundings. The thermal conductivity of a material is measured in Cal/gm/°C/sec [1]. R L Clarke and et al has done a work on Introducing Cerium Based High Energy Redox Batteries, in which for redox battery, Cerium ion was introduced for a high energy positive electrolyte. With the use of good industrial and efficient manufacturing performs, the next goal is to develop this into practical high capacity storage batteries [2]. Some of the researchers have studied the special effects of the addition of rare earth metals (largely lanthanum and cerium) in the eutectic Al-Si alloys. It was found that addition of La or Ce increases the AlSi alloy melting and eutectic temperature, with a recalescence of 2-3°C due to precipitation of rare earth intermetallic, which bases the modification in the crystal structure and the corresponding entropy changes. The partial modification of eutectic Si particles is caused by the addition of La or Ce to Al-(7–13) %. [3]. The work done by David Weiss describes the progress and the castability of near eutectic Aluminum Cerium (Al-Ce) alloy structures. These alloys have worthy mechanical properties and are very castable at high temperatures. In alloy systems, when Si, Mg and /or Cu are added in combination with Cerium, the casting characteristics are better than the Aluminum-Copper system. The mechanical strength at room temperature can be increased by addition of Magnesium [4]. A microstructural refinement can be brought about by addition of Ce below 2 wt%. A decrease of **α**-Al grain size, refining eutectics and morphological variations in unfavourable shape of intermetallic compounds can be brought about by addition of Ce. For most of the cast commercial grades alloys such as Al–Si, Al–Li and Al–Mg the positive effects are observed. The optimum Ce addition is required to get the desired effects. For AlCu alloy system, the slight deviation in the Cerium addition can cause detrimental effects, where Ce delays precipitation of strengthening phases. The thermal stability of Al alloys at high temperature can be improved by addition of Cerium. During early days the research was done on the Al–Si–Ce, Al–Ni–Ce, Al–Cu–Ce alloys and powder metallurgy Al–Fe Ce alloy with Ce content up to 16 wt%. But in the recent decade, there is a re-established interest in using Ce as the major alloying element and research focus on Al–Ce–Si–Mg with Ce exceeding 10 wt% and Al–Cu–Ce alloys with 3–7 wt% Ce [5]. The refinement of the primary silicon and of the eutectic silicon morphology was achieved with additions of cerium (up to 1 % Ce) to hypereutectic Al-Si alloys. With the addition of 1 % Ce, the best results for the microstructural and strength properties were

obtained. With an increase in the cerium additions, the precipitation temperature of the primary silicon phase decreased. The addition of 1 % Ce produced the highest reduction in the liquidus temperature, from 686.6 °C to 591.9 °C [6].

Based on the above literature survey, this project focus on the observation in the electrical and thermal conductivity of Aluminium cerium alloy with varying Ce% and its correlation with the microstructure.

2 Experimental:

2.1: Alloy Preparation:

AlCe10% alloy was made by melting route in a 20kW resistance furnace of 10 kg capacity by adding Ce MM metal (A typical composition includes approximately 55% Ce, 25% La, and 15-18% neodymium with other rare earth metals are seen as a series of 17 elements: scandium, yttrium, and the lanthanide series (lanthanum, cerium, praseodymium, neodymium, promethium, samarium, europium, gadolinium, terbium, dysprosium, holmium, erbium, thulium, ytterbium, and lutetium) following[19]) with argon purging and degassing by Nitrogen. To this AlCe10% alloy, EC grade (99.97% purity) was added subsequently to cast AlCe8%, AlCe4%, AlCe2% and AlCe1% alloy by above mentioned production process. The alloys were cast in to sand casting mould with no shrinkage and blow holes casting defects.

The chemical composition of the alloys is as shown in Table 1:

Table 1: Chemical composition of AlCe alloys

AlCe Alloy	Ce%	La%	Nd%	Fe%	Others%	Al %
Alloy 1	8.63	3.673	0.0265	0.165	0.3138	Balance
Alloy 2	4.91	2.046	0.0166	0.137	0.3245	Balance
Alloy 3	2.80	1.181	0.0083	0.110	0.2987	Balance
Alloy 4	1.92	0.548	0.0045	0.095	0.3167	Balance

The alloy samples were machined with required dimensions for further study.

2.2: Metallography Characterisation and Electrical conductivity measurement:

For metallography analysis the samples were cut, hot mount and mirror polishing (0.5 µm) by LECO machines. For conductivity in % IACS the samples were machined with diameter 40 mm and thickness

8-10 mm and conductivity was calculated by Technofour conductivity meter, Type 979, which works on the principle of eddy currents.

2.3: Thermal Conductivity:

The Searle's apparatus to measure the thermal conductivity of a solid is shown in Figure 1. The alloy is taken in the form of a cylindrical rod AB (Diameter 1.8 cm and length 18 cm). One end A of the rod is kept at a temperature of 2-4°C by passing water from a tube with constant flow rate. Another tube is fitted at the other end B of the rod. The flow of water is adjusted using pinch cork such that water comes drop by drop from the exit side. Water enters the tube at end A away from the chilled water source and it leaves at the end B. Thermometers T3 and T4 are provided to measure the temperatures of the outgoing and incoming water. The whole apparatus is covered properly with layers of an insulating material like wood and glass wool, so as to prevent any loss of heat from the sides. The end A of the alloy rod is kept at temperature of 100°C and 5 calibrated thermocouples were inserted at various places in the rod at equidistance to measure the heat loss from end A to end B. The temperatures of all the thermocouples raise initially and ultimately become constant when the steady state is reached. The readings $\theta 1$, $\theta 2$, $\theta 3$ and $\theta 4$ are noted in steady state.

The whole procedure is repeated for all the other AlCe alloys with different Ce% to observe the effect of various Ce% on the thermal conductivity.

Figure 1: the experimental set up for Thermal Conductivity by Searle's method

Formula Used:

The coefficient of Thermal Conductivity K for a material is given by

$$K=\frac{md\,(\theta_3-\theta_4)}{A\,(\theta_1-\theta_2)}\ \text{cal/gm./°C/sec} \qquad (1)$$

Where A = Area of cross section of the rod ($\pi r2$ where r is the radius of the copper rod (D/2)

$\theta 1$ & $\theta 2$ = Steady temperatures at the two fixed point of the rod in steady state.

d = Distance between two thermometer T1 and T2

m = Mass of water collected per second

$\theta 3$ & $\theta 4$ = Steady temperatures of water at exit and at entrance respectively.

3. Results and Discussions:

3.1: Metallography analysis:

The initial study of the AlCe system is done by phase diagram by Thermo-Calc, Figure 2 [7]. It has a eutectic composition at about 10 wt% Ce with a eutectic temperature of 640°C. Hypo- and hyper-eutectic alloys contain the intermetallic compound Al11Ce3. The evaluation of the castability, microstructure, mechanical

and physical properties of Al-12Ce, Al-12Ce-0.4 Mg, and Al-12Ce-4Si-0.4 Mg alloys were done by Sims et al [8].

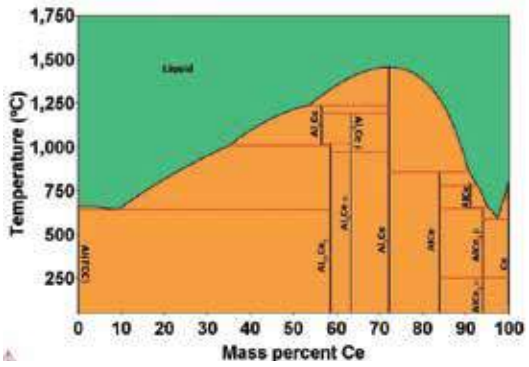

Figure 2: Thermo-Calc calculated Al-Ce phase diagram.

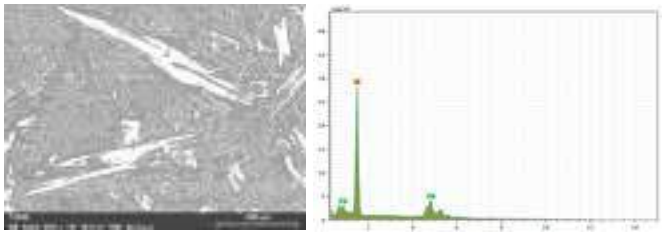

Figure 3: SEM EDS analysis of AlCe8% alloy displaying the presence of large crystals of intermetallic compound $Al_{11}Ce_3$. (Normal mass % of Al: 52.44 and Ce: 47.56)

AlCe alloy (Ce%)	10X magnification	20X magnification	Avg. Grain Size (µm)
8.63			Phase size= 9-183 µm
4.91			Cluster of smaller grains of size 71-95 µm forming bigger grains of size 290 µm
2.80			115 µm
1.92			77 µm

Figure 4: SEM micrographs of AlCe alloys of 8%, 4%, 2% and 1% at 10 and 20X magnification

Among the various AlCe alloys containing 8%, 4%, 2% and 1% Ce, the first belong to the hypoeutectic group and remaining three alloys to the hypereutectic group. AlCe8% displays the presence of large crystals of intermetallic compound $Al_{11}Ce_3$ [5]. The presence of $Al_{11}Ce_3$ is confirmed by EDS analysis as per Figure 3.

The SEM micrographs of AlCe alloys of different Ce% are shown in the following Figure 4 at 10X and 20X magnifications. By contrast, a very fine interconnected eutectic microstructure is apparent for the hypoeutectic Al-4%, AlCe 2% and AlCe 1% alloy.

From the above Figure 4 it shows that with lowering the Ce% from 8% to 1% there is decrease in the grain size of alloy. AlCe8% alloy shows the presence of large intermetallic and no grain formation. AlCe4% alloy has the grain size of 290 µm whereas for AlCe2% and AlCe1% it is of 115 µm and 77 µm respectively. The efficiency of Ce has been established for the Al– 20Si alloy, where 0.3, 0.5, 0.8 and 1.0 wt% Ce led to a substantial refinement of primary Si crystals through morphology alteration from coarse polygonal and star like forms to fine blocky forms with smooth edges and corners [6, 9].

3.2: Electrical conductivity:

The benefits of Ce additions to improve tensile strength and elongation of aluminum at room temperature were carried out by earlier researcher by adding up to 0.1 wt% Cerium [10]. The negligible cerium additions used in widely held of experiments are below 1 wt%; only in nearly cases they reach 2 wt%.

According to the various researchers, Ce additions advance electrical conductivity of Al alloys due to a decrease of Fe and Si in the **α**-Al solution. The solvent content reduction is accredited to the development of binary, ternary or quaternary complexes of Ce, Si, Fe and Al [11, 12, 13]. It is believed that Ce increases the lattice static distortion of Al alloy solution and enlarges the average electrical free path. As a result, Ce-influenced alteration of electron energy band structure may exaggerate the operational number of electrons that participate in conduction [14]. Consequently, electrical conductors are produced from Al-based alloys with additions of 0.55 to 1.2 wt% Fe and 0.2 to 1.5 wt% Ce [15].

In this experiment the electrical conductivity was measured in terms of % IACS for all the four alloys of AlCe as mentioned above. The variation in the %IACS was observed and noted in Figure 5.

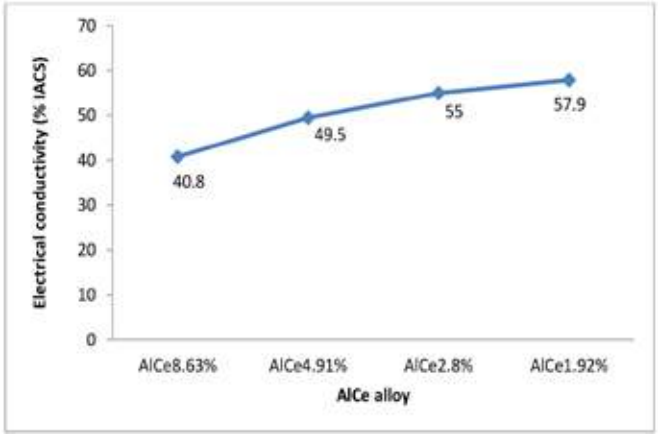

Figure 5: % IACS for AlCe alloys for various Ce%

From the above table it was observed that with decreasing the Ce% from 8% to 1% the electrical conductivity has increased. For AlCe8% alloy it is 40.8 %IACS and for AlCe1% it is 57.9 %IACS. This increase in the conductivity with decreasing Ce% is in correlation with the microstructural changes as observed in the Figure 4 and alteration of electron energy band structure.

The alloying elements having comparable electronic structure to that of aluminum can be least detrimental to conductivity. The rare earth elements, such as Ce have comparable electronic arrangement, in the solution in an aluminum matrix; yield a very low distinction change in the resistivity of aluminum this gives the greatest bonding with the largest free energy [16, 17].

3.3: Thermal Conductivity:

The thermal conductivity was determined by Searle's method as mentioned in the experimental section in terms of Cal/gm/°C/sec. Earlier studies on binary Al-Ce alloys demonstrate enhanced thermal strength at high temperatures for various claims. Therefore, the main objective of the current work is to comprehend the effect of alloying elements and correlate the microstructure-electrical conductivity-thermal stability of Al-Ce. In this experiment the thermal conductivity was determined from 4°C to 100°C.

Earlier work done by Dheeraj Kumar Saini and et al [18] studied the effect of thermal stability of AlCe12% alloy in various Al-Si-Mg alloy with and without Strontium addition at 200 – 400°C. The Al11Ce3 intermetallic phase, provides the strength and thermal stability to the alloy, has a microstructure that comprises at least one of the lath structures and rod morphological structures [6]. Elements in the solution are least harmful to conductivity if they have comparable electronic structure to that of aluminum. The rare earth elements, such as Ce have comparable electronic arrangement, in the solution in an Al matrix, produce a very little differential alteration in the resistivity of Al this gives the best bonding with the major free energy [17]. Work has been done by many researchers on effect of Ce addition in AlSiCu alloy, but here the work is presented on the effect of various % addition of Ce in EC grade Al (99.7% purity). According to M Song [4, 3], Ce improved the thermal stability of the Al-Cu-Mg-Ag alloy by reducing the diffusion velocity of Cu atoms and growing the energy barrier of the coagulating ledge nucleation thus improving the strength of the alloy at both room and raised temperatures. In this work, initially the thermal conductivity was calculated for pure Al to prove the correctness of the assembly done and it came out to be 0.516736 Cal/gm/°C/sec which was matching with the theoretical one. After this the same experiment was carried out for AlCe alloys with various Ce%. The value of thermal conductivity is as shown in Table 2.

Table 2: Thermal conductivity in cal /cm sec. K for AlCe alloy with difference Ce%

Al alloy	Δm (ml)	Δt(s)	ΔT water	ΔT Bar	Coefficient of thermal conductivity (Cal/gm/°C/sec)
Pure Al	59	193	17	61.3	0.516736
AlCe 8.63%	60	191	13	57	0.44514
AlCe 4.91%	60	193	14	58	0.466235
AlCe 2.80%	59	215	16	57.8	0.483921
AlCe 1.92%	61	206	15	52	0.480331

The thermal conductivity was found to be in the increasing order with decreasing Ce%. But for AlCe2% and AlCe1% there is a very little difference in the thermal conductivity as there is only 1% difference in the Ce% which is not sufficient to quantify the thermal conductivity variance. The thermal and electrical conductivities (Figure 5) has a good correlation with respect to the Ce% which is also has the association with grain refinement of AlCe alloy with decreasing Ce%. The more fines are the grains which is making it more thermally and electrically stable system.

The thermal stability of AlCe binary alloy is connected with Al-$Al_{11}Ce_3$ eutectic phase with melting point of 1251°C. However, the Al11Ce3 eutectic phase with lamellar morphology offers limited strengthening to the alloy [19, 20, 21]. The further improvement in the thermal conductivity of AlCe alloy can be brought about by another alloying element such as Nickel, having the diffusion coefficient in aluminum lower by about four orders of magnitude than that for Ni [21]. According to recent statements [19, 22], alloying with Ce aided holding the mechanical properties of Al alloys at higher temperatures than that seen in Ce–free Al alloy grades. After introductions to temperatures as high as 500°C for 1000 hours, Al–Ce displays widespread hardness recovery at room temperature.

Conclusion:

Cerium was added with increasing % into EC grade Al alloy to observe the effect on metallography, electrical and thermal conductivity. The refinement in the microstructure was observed with decreasing Ce%. The more fine grains of 77 µm were observed with AlCe1% alloy. This alloy with Ce1% was observed to have highest electrical (57.9%IACS) and AlCe2% alloy with maximum thermal conductivity (0.48 cal /cm sec. K) among other AlCe alloys. The difference in the thermal conductivity with AlCe2% alloy and AlCe1% alloy was very slight due to its comparative microstructural and corresponding electrical conductivity parameters. AlCe1% alloy and AlCe2% alloy are the future promising alloys for battery applications due to its enhanced thermal and electrical parameters for AlSi, AlSiCu, AlSiMg alloys.

STILL GUESSING
WHERE METAL PRICES WILL GO IN 2021?

DON'T! Just **HEDGE** using **BASE METAL** delivery-based futures contracts on domestic commodity derivatives Exchanges!

ALUMINIUM | COPPER | LEAD | NICKEL | ZINC

MCX
METAL & ENERGY
Trade with Trust

MCX INVESTOR PROTECTION FUND

Issued in Public Interest by Multi Commodity Exchange Investor Protection Fund
Read the Risk Disclosure Document (RDD) carefully before transacting in commodity futures and options

WWW.MCXINDIA.COM

Acknowledgments:
The authors gratefully acknowledge the Department of Physics, Dharampeth Science College (DSC), Nagpur, MH for providing the immense laboratory support in establishing the set up for Searle's Experiment in determining the Thermal Conductivity.

Future Scope of work:
Study the electrical and thermal conductivity of Al-Ce alloys with Silicon, Magnesium and Copper addition at elevated temperature (200-500°C) with and without annealing and correlate it with its mechanical and microstructural properties.

References:

1. Top 10 Thermally Conductive Materials - Thermtest Inc
2. R L Clarke, S. Harrison, B. J. Dougherty, S. Mohanta, J.P. Millington, "Introducing Cerium Based High Energy Redox Batteries"
3. M. Song, D. Xiao, and F. Zhang, "Effect of Ce on the thermal stability of the Ω phase in an Al-Cu-Mg-Ag alloy," Rare Metals, vol. 28, no. 2, pp. 156–159, 2009
4. David Weiss, "Castability and Characteristics of High Cerium Aluminum Alloys", Advanced Casting Technologies, Intech Open
5. Frank Czerwinski, Hamilton, "Cerium in aluminum alloys", Canmet MATERIALS, Natural Resources Canada, , Canada J Mater Science Review
6. Stanislav Kores, Maja Vonina, Borut Kosec, Primo` Mrvar, Josef, "Effect of cerium addition on the AlSi17 casting alloy", Medved, Materiali in tehnologije , Materials and technology 44 (2010) 3, 137–140
7. Weiss D, Rios O, "Low density and temperature tolerant alloys for automotive applications", March 2017 SAE International, 2017-01-1666
8. Sims ZC, Weiss D, McCall SK, McGuire MA, Ott RT, Geer T, Rios O, Turchi PAE, "Cerium based, intermetallic-strengthened aluminum casting alloy: High-volume co-product development", Journal of Materials. 2016;68(7):1940-1947
9. Li Q, Xia T, Lan Y, Zhao W, Fan L, Li P, "Effect of rare earth cerium addition on the microstructure and tensile properties of hypereutectic Al–20%Si alloy", J Alloys Compd 562(1): (2013) 25–32
10. Barth O (1912) Metallurgie 8:261
11. Alkahtani S, Elgallad E, Tash M, Samuel A, Samuel F, "Effect of rare earth metals on the microstructure of Al–Si based alloys", Materials 9(45): (2016) 1–13
12. Li P, Wu Z, Wang Y, Gao X, Wang Z, Li Z, " Effect of cerium on mechanical performance and electrical conductivity of aluminum rod for electrical purpose", J Rare Earths 24(1): (2006) 355–357
13. Wilka VC, "Aluminum cerium iron electrical conductor and method for making same" US Patent 3 964 935, 22 June 1976
14. Liao H, Liu Y, Lu C, Wang Q, "Effect of Ce addition on castability, mechanical properties and electric conductivity of Al–0.3Si–0.2Mg alloy", Int J Cast Met Res 28(4): (2015)213–220
15. Wilka VC, "Aluminum cerium iron electrical conductor and method for making same", US Patent 3 964 935, 22 June 1976
16. Study the Effect of some Metallic Additives on the Physical Properties of the Commercial Pure Aluminum Metal E.M.Sakr, A.Nassar, N.Tawfik and M.Soliman, Journal of American Science 2010;6(12)
17. L. Brewer, P. Rudwan, J. Striger, R. I. Jaffe, "Phase Stability in Metals and Alloys", McGraw-Hill Book Co., N.Y., (1967)
18. "Effect of alloying elements on thermal stability of Aluminium-Cerium based alloys", Research Square, https://doi.org/10.21203/rs.3.rs-67587/v1)
19. Frank Czerwinski, "Thermal Stability of Aluminum Alloys", Materials 2020, 13, 3441; doi:10.3390/ma13153441
20. Czerwinski, F. Shalchi Amirkhiz, B. "Al-Al11Ce3 eutectic transformation in aluminum-cerium binary alloys", Metall. Mater. Trans. A 2020, in press
21. Czerwinski, F. Cerium in aluminum alloys. J. Mater. Sci. 2020, 55, 24–72
22. Weiss, D. "Improved high temperature aluminum alloys containing cerium", J. Mater. Eng. Perform. 2019, 28, 1903–1908

PELEE'S ALUMINUM WINE BOTTLES BLOSSOM

Pelee Island Winery expands its packaging options with a 250-mL aluminum bottle for its Lola series that mimics the grace and beauty of its glass bottle counterpart.

The 250-mL aluminum bottle is a stock package from Trivium that is direct printed in up to six colors and is topped with a silver screw cap.

With its graceful, tapered-shoulder silhouette and stunning floral artwork, a new 250-mL bottle from Pelee Island Winery for its Lola line of four wine varieties artfully brings the aesthetics of a traditional wine package to an aluminum bottle format. Introduced initially in Ontario, Canada, the bottle and brand extension generated considerable buzz among the winery's retail and on-premise partners as well as excitement from Pelee's loyal followers when it was launched in spring 2021.

Each variety of Lola in the new aluminum bottle is variety decorated with a floral pattern that matches the label used for its 750-mL glass bottle counterpart.

EFFECT OF NA-GLASS DISPERSION ON IONIC AND ELECTRONIC TRANSFERENCE IN Ag_2SO_4

J.B.Randhawa[1] and P.W.Ambekar[2]
[1]Government College of Engineering, Nagpur (India) 441108.
[2]Dharampeth M P Deo Memorial Science College, Nagpur (India)
pacific0701@gmail.com

ABSTRACT

In the present study composite electrolytes of Ag_2SO_4 were prepared by dispersing high T_g Na-glass in different compositions. Formation of glass and composite was confirmed by powder X-ray diffraction study. Ionic and electronic conductivity measurements were carried out using Complex Impedance Spectroscopy and Wagner's dc polarization technique respectively. Nyquist plot reveals two different conduction mechanisms in the composite Ag_2SO_4+glass for all composition. Two orders of enhancement in ionic conductivity were observed at lower temperatures. The phase transition temperature of Ag_2SO_4 is found shifting to lower temperature side on increasing dispersoid concentration. DC conductivity study revealed that for pure Ag_2SO_4, $\sigma_{ion} > \sigma_{ele}$ and the electronic conduction is via both electrons and electron-holes, in agreement with earlier reported data. Electron-hole transference number is found more than the electron transference number indicating domination of p-type conductivity in pure phase. On the contrary Ag_2SO_4+glass composite showed n-type electronic conductivity. For a SO_2 gas sensor with cell configuration: $Ar,O_2,SO_2,Pt/Ag_2SO_4/Ag$(sealed); at high silver potential, silver ions are incorporated into the lattice of electrolyte and for neutrality reasons, the concentration of excess of electrons (e') in solid is increased. Performance of a typical SO_2 gas sensor is discussed in light of above conductivity results.

Keywords: *Composite, Electrochemical Gas Sensor, Electronic Conductivity, Solid Electrolyte, Wagner's DC polarization technique*

1. Introduction

With the advancement of nanotechnology major thrust is being given on development of solid-state gas sensors (semiconductor type) for their fast response and miniaturized dimensions. Yet a reliable SO_2 gas sensor with high selectivity is to be developed (Beatty et al, 2014; Hunter et al, 2020). Electrochemical gas sensors overcome the major disadvantages associated with solid state sensors, as they are highly selective and follows a theoretical relation which obviates the need of calibration. In the present study effect of electronic conductivity of the electrolyte on performance of an electrochemical SO_2 gas sensor is studied.

The electrochemical devices viz., batteries, fuel cells, sensors, super-capacitors *etc*. use solid electrolyte as a prime component. The electrolyte should possess fast ionic transference with negligibly small electronic conductivity. Enhancement in ionic conductivity of solid electrolyte is obtained either by iso/aliovalent doping, making solid solution or composites. The first crystal-crystal composite solid electrolyte has been obtained with sub-micron size alumina particles dispersed in Lithium Iodide matrix, exhibiting 50 times higher Li-ion conductivity at room temperature in relation to the host (Liang, 1973). Since then, a large number of composite solid electrolyte have been reported by dispersion of insulating phase e.g. α,β,γ-Al_2O_3, SiO_2, α-Fe_2O_3, MgO, Fly-ash, ZrO_2 into pure solid ionic conductor viz. LiBr, LiCl, CuCl, AgI, HgI_2, CaF_2, AgCl, Li_2SO_4, Ag_2SO_4, Na_2CO_3, glasses *etc*. Composites are preferred for device applications due to their inherently advantageous characteristic properties such as high ionic conductivity at relatively low temperatures, homogeneity in electrical and mechanical properties, better interface with electrode/s, enhanced electrode kinetics and stable thermal properties.

Ag_2SO_4 is an apt candidate for electrolyte/test electrode application in an electrochemical SO_2 gas sensor due to various advantages viz. high ionic conductivity with low activation enthalpy, non-hygroscopic nature, coexistence of Ag-Ag_2SO_4 as an equilibrium phase, better sinter ability etc. (Singh and Bhoga, 1999). The major disadvantage associated with pure phase sulfate-based electrolyte system is its very poor mechanical strength, porosity and instability over thermal cycling. The SO_2 sensors have Ag+Ag_2SO_4 as reference electrode. This reference electrode needs

sealing from the test gas. Pure Ag_2SO_4 or its heterogeneous composite electrolyte failed to give proper sealing because of large difference in thermal expansion coefficient of reference electrode and that of the electrolytes. In order to overcome these limitations glass bonded Ag_2SO_4 electrolytes with different compositions were prepared.

In the present study glass dispersed composite electrolytes was prepared by dispersing high t_g Na-glass ($Na_2O+2B_2O_3+7SiO_2$) into Ag_2SO_4 in different compositions. Looking at the necessity of high operating temperature of SO_2 gas sensor, a non-conducting glass with high glass transition temperature (>550°C) was selected for dispersion. Formation of glass as well as composite was confirmed by powder x-ray diffraction study. Electrical characterization i.e. ionic and electronic conductivity measurements were carried out using complex impedance spectroscopy and Wagner's DC polarization technique respectively.

2. Experimental

2.1 Preparation of Glass

Na^+-glass of composition $10Na_2O:20B_2O_3:70SiO_2$ were prepared by rapid melt quenching. Well-dried initial ingredients Na_2CO_3, H_2BO_3 and SiO_2 having purity > 99.98 % were taken in an appropriate mole ratio. Mixed under acetone for an hour and then subjected to calcification in a porcelain crucible above the decomposition temperature of Na_2CO_3 (900°C) for converting into Na_2O and CO_2 gas (evolved). The temperature of the mixture was then raised to its melting, and the melt was soaked for an hour at the melting temperature (1100°C) for homogenization. The melt was quenched to room temperature between two flat surfaced Aluminum blocks. The quenching rate offered by the Aluminum blocks was 100°C/s (Singh and Ratnam, 1988). The glass formed was found to be transparent. These glass flakes were crushed and sieved to get fine powder (<40μm) for dispersion into Ag_2SO_4.

2.2 Glass Dispersed Composite

Fine powder of Na^+ glass was mixed with well-dried Ag_2SO_4 in the composition $(100-x)$ Ag_2SO_4: (x) glass, (where x = 0, 5, 10, 15 & 20 weight %). The compositions were mixed manually under acetone for an hour. The dried materials were then palletized (D = 9mm and t = 1-2mm) and kept in a programmable furnace. The temperature of the furnace was raised to 550°C and kept at this temperature for 2 hr followed by slow cooling (furnace cooling) to room temperature. Very sturdy and compact pellets of the composite were obtained without change in the color or form. This compactness was expected to result because of lowering of glass softening temperature due to palletization. The melted/soften glass helps in filling the pores between the grains of pure sulfate phase as well as tries to glue them together.

2.3 Impedance measurement

Glass dispersed composites was palletized in the form of circular discs of dimensions approximately 9 mm in diameter and 1-2 mm in thickness by pressing uniaxially at pressure 4 tons/cm^2 using stainless steel die-punch and hydraulic press (Specac UK). Later, the pellets were sintered at 773K for 6 hours. A thin film of Silver was painted on both the flat surfaces of pellet to ensure good ohmic contacts. Six samples were loaded simultaneously between silver electrodes of specially designed sample holder. The computer-automated system was used for multi-channel complex impedance measurement using Impedance analyzer (HP 4192A).

2.4 Electronic and ionic transport measurement

Transport number measurement of Ag_2SO_4 and Ag_2SO_4+glass was carried out at 723K. This temperature was selected because it is well above the transition temperature (690K) of Ag_2SO_4 from β to α phase. The SO_2 gas sensors are operated at temperature above 773K.

The sample was placed between the two pressurized gold lids sample holder. The cell configuration for transport number measurement in ambient gas atmosphere is given as

Ag, O_2, Ar (-)/ Ag_2SO_4 / (+) Ar, O_2, Pt

The schematic of experimental set-up used for measurement is shown in figure (1). The sample while mounted in a sample holder was

heated up to 725K and maintained at this temperature for entire measurement of transport number using Eurotherm temperature controller (±1°C). After attaining thermal equilibrium, a d.c. potential was applied with the help of source and measure instrument (Keithley SMU236) and recorded simultaneously the current through sample as a parametric function of time. The data was stored by interfacing the instrument to IBM PC through indigenously developed software. The sample was allowed to get polarize by maintaining the identical temperature and potential in ambient atmosphere.

Fig. 1: Schematic representation of DC. polarization cell. The reversible electrode Ag exchanges both cations Ag^+ and electrons.

3. Results and Discussion

The x-ray powder diffraction pattern for $10Na_2O+20B_2O_3+70SiO_2$ glass is shown in figure (2). A broad diffused scattering over several degrees suggests lack of regular crystalline structure hereby confirming its amorphous nature. The x-ray powder diffraction pattern of Ag_2SO_4 dispersed with glass of above composition is shown in figure (3). All the major peaks correspond to Ag_2SO_4. No other major crystalline phase was observed that would have resulted on reaction of Ag_2SO_4 with glass

.

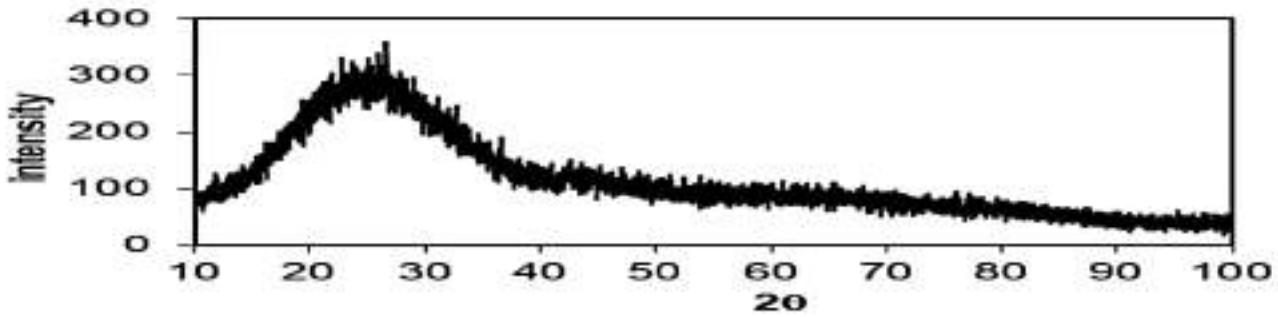

Fig. (2): Powder XRDpattern for $Na_2O+2B_2O_3+7SiO_2$ glass.

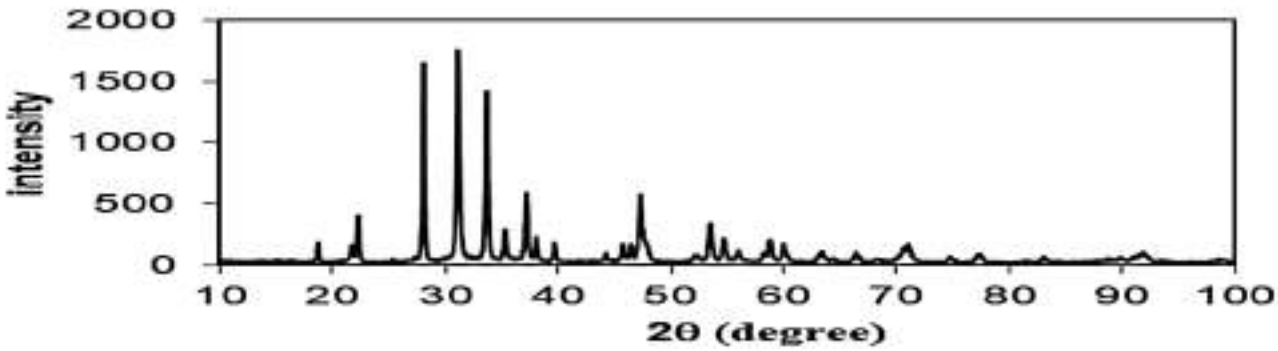

Fig. (3): Powder XRD pattern for $Na_2O+2B_2O_3+7SiO_2$ glass dispersed Ag_2SO_4.

Typical impedance curves for the composite $0.8Ag_2SO_4+0.2(10Na_2O+20B_2O_3+70SiO_2)$ of composition at two different temperatures is shown in figure (4), revealing the presence of two overlapping depressed semicircular arcs suggesting two different conduction regimes within the material. Two major pathways taking part in the conduction are Ag_2SO_4/glass interface and the bulk of Ag_2SO_4 grains (Singh, 1993). The surface interaction at Ag_2SO_4/glass-heterojunction is described analogous to one at the moderately ion conductor/insulator interface giving rise to a space charge layer (Maier, 1985). The type of interface interaction could not be revealed here because of limited frequency range of measurement, which restricted formation of high frequency semicircle at higher temperatures

.

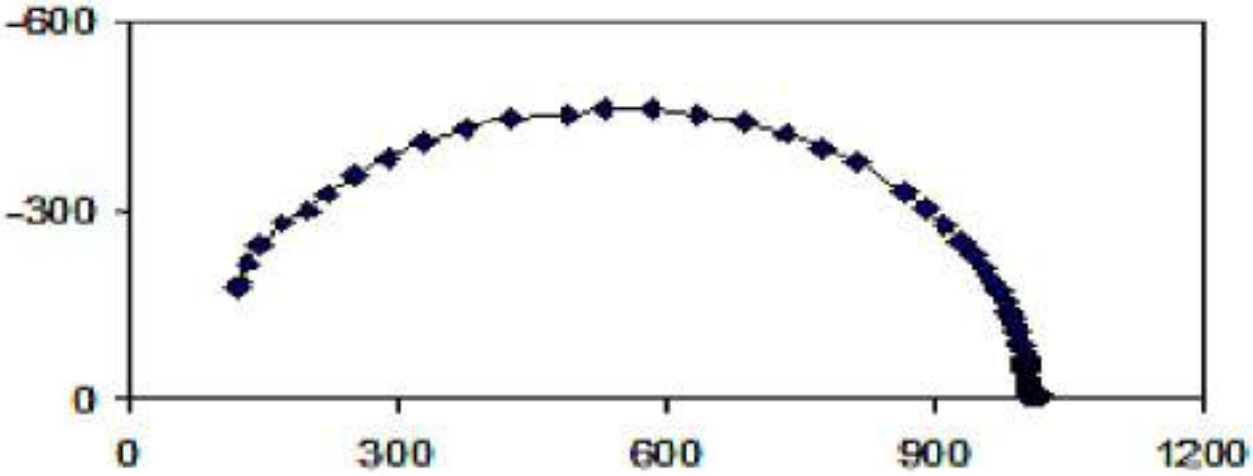

Fig. 4 (a & b): Complex impedance plots for $0.8Ag_2SO_4+0.2$glass at 660 and 610K.

The total resultant conductivity was determined from the real axis intercept of the complex impedance plot. Figure (5) shows that conductivity of Ag_2SO_4 and its glass-dispersed composite obey the Arrhenius law over the entire temperature range of investigation. Large conductivity enhancement is observed due to glass dispersion over complete range of temperature with more predominance at lower temperature. The magnitude of conductivity at higher temperatures is same as that of the pure Ag_2SO_4. The phase transition temperature of Ag_2SO_4 from orthorhombic β-phase to hexagonal α-phase is affected by the dispersoids addition. This is a typical of heterogeneous composite electrolytes (Chowdhari, Tare and Wagner, 1985). For most of the composites it has been observed that a hysteresis in Arrhenius plot is seen on taking the conductivity measurement while heating and cooling the sample (Shahi and Wagner Jr., 1981; Chowdhari, Tare and Wagner Jr., 1985). The transition temperature has been found unaffected while conductivity is measured on heating but found decreasing while cooling the sample. The decrease in transition temperature was found proportional to the dispersoids content. This decrease in α to β transition temperature has been explained on suggestion that the interaction of cation interstitials with the strain field associated with the volume charge is the principal factor responsible for the phase transition (Rice, Strassler and Toombs., 1974). This significant result is observed while cooling because of existence of large no of thermally generated defects. The decrease in transition temperature ΔT has been reported to be linearly proportional to content of second phase. Similar results were obtained in the present study.

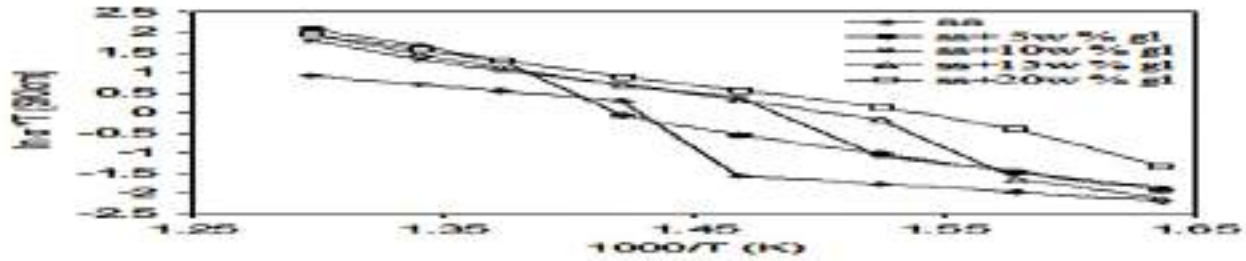

Fig. 5: Arrhenius plots for Ag_2SO_4 +glass composite electrolyte of the compositions mentioned. ss: Ag_2SO_4, gl: glass

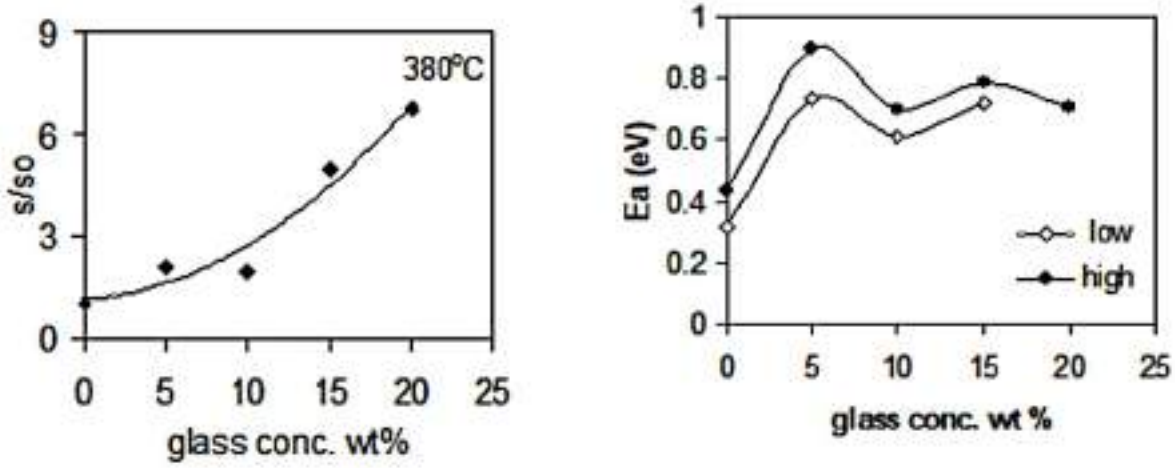

Fig. (6a): Conductivity enhancement as a function of glass concentration (6b): Variation in activation energy E_a with glass concentration.

The variation of conductivity enhancement σ/σ_o at 380°C and activation enthalpy before and after the phase transition with weight fraction of dispersoid glass is depicted in figs. (6a and b) respectively. Fig. (6a) reveals that the conductivity continuously increases with glass content instead of a sharp one as predicted from percolation theory for composite solid electrolyte (Jiang and Wagner Jr., 1995). Such conductivity behavior may be due to relatively larger surface area of interaction of dispersed phase with the host grains, whereas, percolation threshold is obtained for fine particle (sub-micron) dispersion. Higher concentrations of glass dispersion were not tested because the electrolyte to be developed was required to be necessarily of Ag_2SO_4 in SO_x gas sensors. As $Ag+Ag_2SO_4$ reference electrode gives thermodynamic stability as well as complete reversibility with Ag_2SO_4 electrolyte. Increased glass content in the electrolyte is likely to disturb this equilibrium.

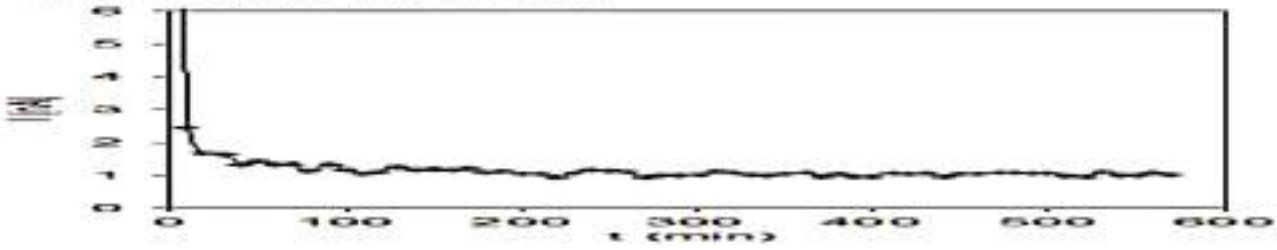

Fig.7: Polarization curve for Ag_2SO_4 at polarizing potential of 0.22V at 723K.

Typical time variation of polarizing current on application of a small DC potential is shown in figure (7). The initial large current is due to motion of ions as well as electrons while a constant current was observed after polarization of ions, and this conductivity is due to electronic charge carriers alone. The equilibrium value of this steady current was obtained by taking average of last steady state observations as shown in the inset. In order to get the preliminary ideal of the potentials required for polarization the voltage was applied in larger steps and general trend of the voltage-current characteristic for pure Ag_2SO_4 was obtained as shown in figure (8a). Later the same set of observations was repeated for another Ag_2SO_4 pellet with smaller variation in polarizing potential. The so obtained V-I characteristic is shown in figure (8b). This typical nature of the *log I* vs polarizing potential *E* curve shows that $\sigma_{ion} > \sigma_{ele}$ and both electron $\sigma_{\ominus}$ as well as hole $\sigma_{\oplus}$ conductivity is dominating in the sample (Wagner , 1956). The magnitude of $\sigma_{\ominus}$ was obtained from the constant current plateau at the potential (E = 0.32V) where sudden increase in current starts for the second set observations (Kopp et al, 1993; Poulsen et al, 1983). Also, the magnitude of hole conductivity $\sigma_{\oplus}$ was calculated from the slope of the curve wherein current increases exponentially with applied potential. The values of electron and hole conductivities were found to be $\sigma_{\oplus} = 1.0059\text{x}10^{-7}$ S/cm and $\sigma_{\ominus} = 8.38998\text{x}10^{-9}$ S/cm respectively. From these conductivities as well as taking total conductivity from ac measurements the hole and electronic transport numbers were calculated as $t_{\oplus} = 1.95\text{x}10^{-4}$ and $t_{\ominus} = 5.54\text{x}10^{-6}$. The current voltage behavior for the composite electrolyte with following cell configuration: (+)Ar,O_2,Pt/Ag_2SO_4+glass/Ag,O_2, Ar (-) at 723K is shown in fig (9). The magnitude of electronic conductivity was calculated from the plateau current as $\sigma_{\ominus} = 1.10797\text{x}10^{-6}$ S/cm and the corresponding transport number $t_{\ominus} = 7.3128\text{x}10^{-4}$. Thus, the preliminary observation shows that the Ag_2SO_4+glass composite has very small n-type electronic conductivity.

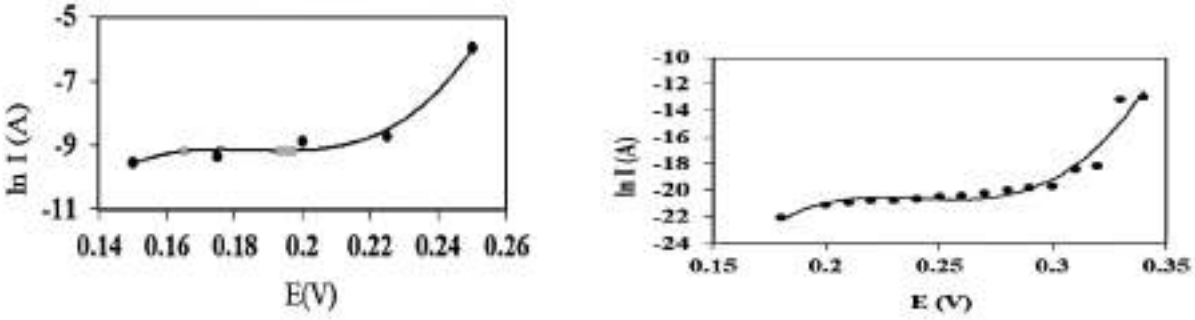

Fig. 8: Current voltage curve of pure Ag_2SO_4 for different sample thickness at 723K

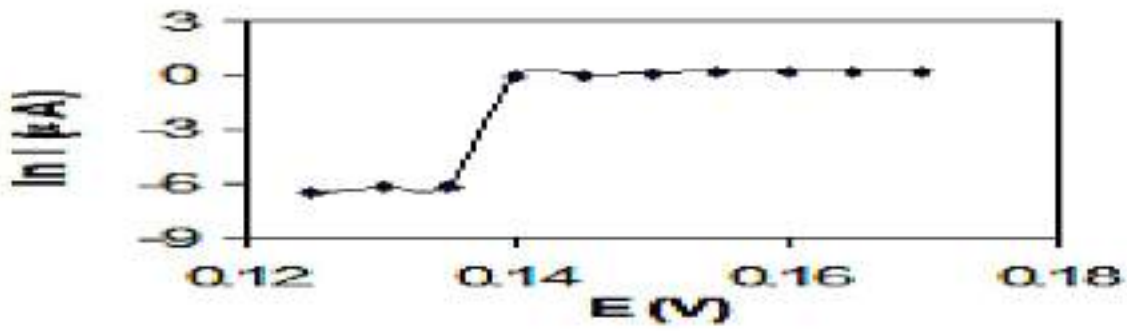

Fig.9: Current voltage behavior of Ag_2SO_4 +glass composite at 723K in ambient atmosphere.

The earlier reported measurement of transport number for pure Ag_2SO_4 (prepared by chemical reaction of $AgNO_3$ with H_2SO_4) at 719K where smaller polarizing emfs (0.04 to 0.14V) have been applied across the pellet of thickness 3mm and dia. 8mm with Ag and Pt as reversible and blocking electrodes respectively (Hauffe and Hoeffgen, 1966). The magnitude of hole transport number calculated using slope of the graph in the linear portion has been reported to be $t_{\oplus} = 1x10^{-4}$ showing predominance of hole conductivity which is in agreement with our observations.

Both p and n-type electronic conductivity was found present in pure Ag_2SO_4 with domination p-type conduction which is in agreement with the earlier reports. The type of electronic conductivity was found changing from p-type to n-type on dispersion of glass. This result for Ag_2SO_4+glass composite is in contrast with other reported composites. Wagner-Hebb polarization of LiI:Al_2O_3 (Liang, Joshi and Hamilton, 1978; Poulsen et al, 1983), AgI:Al_2O_3 (Shahi and Wagner Jr., 1981), AgCl:Al_2O_3 (Maier, 1995) indicate an increase in the p-type conduction with respect to pure material. The effect is very weak in CuCl:Al_2O_3 but the tendency is analogous (Jow and Wagner Jr, 1979).

In electrochemical devices, the electronic charge carriers (electrons/holes) in the electrolyte affect the device performance significantly when operated under open circuit conditions, e.g. an electrochemical sensor in potentiometric mode. The variation in electronic charge carriers under different operating conditions has been explained on the basis of charge neutrality (Nafe, 1994). At high silver potential, silver is incorporated into the lattice of the electrolyte, and hence the concentration of excess of electrons (e') in the solid is increased. This charge balance is totally independent of the exact nature of the defects involved in the incorporation process. Detailed information about the defects can be abstracted by simply regarding the building unit $Ag^{\bullet}$, which characterizes a silver ion dissolved in the solid:

$$Ag \Leftrightarrow Ag^{\bullet} + e'$$

$Ag^{\bullet}$ can be a combination of the structure elements Ag_{Ag} (regular silver site) and V'_{Ag} (silver vacancy)

$$Ag_{Ag} \Leftrightarrow Ag^{\bullet} + V'_{Ag} \quad \text{or}$$

$$Ag^{\bullet} \Leftrightarrow Ag_{Ag} - V'_{Ag}$$

or a combination of $Ag_i^{\bullet}$ (silver interstitial) and V_i (interstitial vacancy)

$$Ag^{\bullet} \Leftrightarrow Ag_i^{\bullet} - V_i$$

Similarly at low silver activity, silver is released from the solid. As a result, electron holes ($h^{\bullet}$) are formed whatever the involved atomic defects are:

$$Ag^{\bullet} \Leftrightarrow Ag + h^{\bullet}$$

The motivation behind taking up the above transference number studies of the Ag_2SO_4 and Ag_2SO_4+glass electrolyte is to investigate reason behind the significant deviation observed in sensor emf from Nernst's law in the SO_2 gas concentration range from *600 ppm* to *13%*, despite showing sensitivity close to the theoretical value. Variation in sensor emf for the cell

$Ar, O_2, SO_2, Pt / Ag_2SO_4 / Ag$ *sealed*

with different test gas concentration at 773K is shown in figure (10). The cell emf of this sensor is governed by the relation

$$E = \frac{-\Delta G^{o}(T)}{2F} + \frac{RT}{2F} \ln \frac{P_{SO_2} P_{O_2}^{1/2}}{a_{Ag_2SO_4}}$$

.....

(1)The magnitude of sensitivity was obtained from the slope of the straight line as 0.028V which is close to the theoretical sensitivity value 0.033V at 773K in the lower test gas partial pressure region (250ppm to 7.8%)

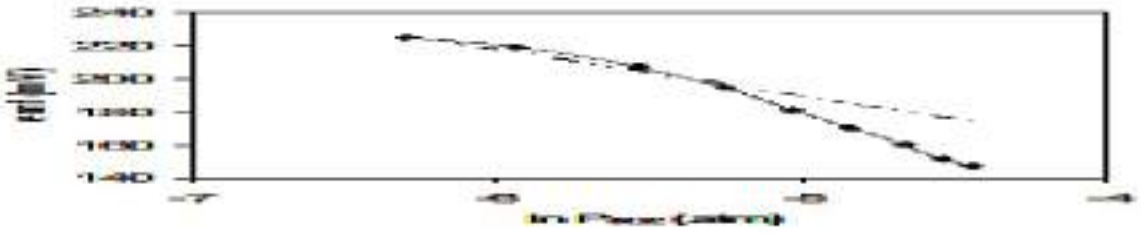

Fig. 10: Variation in sensor emf of cell with SO_2 partial pressure at 773K

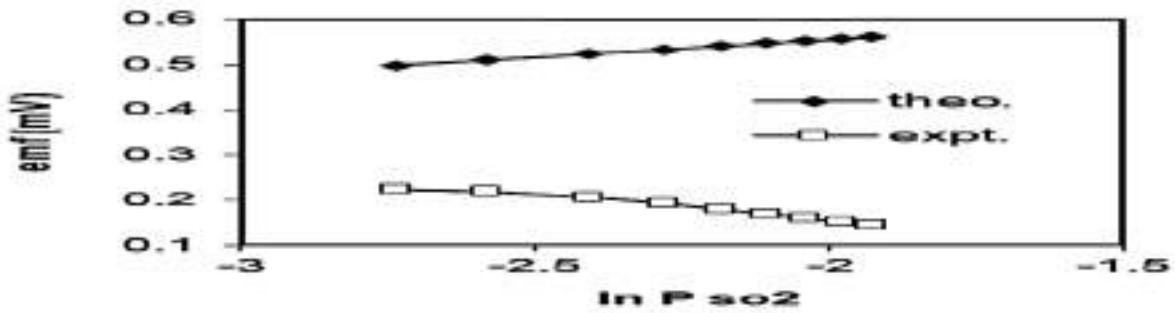

Fig.11: Comparison of sensor emf with theoretically calculated value for the cell at 773K

The theoretical value of sensor emf for above cell configurations calculated using theoretical data (Barin, 1993) for Gibb's free energy of Ag_2SO_4 at 773K and taking a_{Ag2SO4} equal to unity in the $Ag+Ag_2SO_4$. This emf is shown against the experimentally obtained response in figure (11), depicting significant deviation from Nernst law.

4. Conclusion

Two orders of magnitude enhancement in conductivity of Ag_2SO_4 is obtained when a composite is formed by dispersion of Na glass into it. The type and magnitudes of electronic transference number of pure Ag_2SO_4 was found in close agreement with the previous reported values. In the composite, Ag_2SO_4 + glass, n-type conduction is found dominant for the applied voltages up to 0.17V. Wagner's dc polarization study supports mechanism of defects creation at grain boundary interface. The large deviation in the magnitude of sensor emf could not be due to electronic conductivity of the electrolyte as the electronic transport number t_e for Ag_2SO_4+glass electrolyte was obtained of the order of 10^{-4} as seen from Wagner's polarization results for this electrolyte.

5. Acknowledgements

Authors are thankful to Department of Physics, RTM Nagpur University for providing experimental facilities.

References

1. Barin Ihsan, (1993). Thermodynamical Data of Pure Substances, VCH, Stuttgart.
2. Beatty B., Braus G., Durbin L., Eickhoff J., Fiehweg B., Ray M., Ryon T., Schlomberg K. and Schmitz E. (2014). Environmental Performance Report, https://www.nrel.gov/docs/fy15osti/64208.pdf
3. Chowdhari P., Tare V.B. and Wagner J. B. Jr, (1985). Electrical Conduction in AgI - Al_2O_3 Composites, J. Electrochem. Soc. Vol.132(1), pp. 123-124.
4. Hauffe K. and Hoeffgen D., (1966). Z. Physik Chemie, 49 94-111.
5. Hunter Gary W., Akbar Sheikh, Bhansali Shekhar, Daniele Michael, Erb Patrick D., Johnson Kevin, Liu Chung-Chiun, Miller Derek, Oralkan Omer, Hesketh Peter J., (2020). A Critical Review of Solid State Gas Sensors, *J. Electrochem. Soc.* Vol.167, pp. 037570.
6. Jiang S. and Wagner J. B. Jr., (1995). A theoretical model for composite electrolytes—II. Percolation model for ionic conductivity enhancement, J. Phys. Chem. Solids, vol. 56(8), pp. 1113-1124.
7. Jow T. and Wagner J. B. Jr., (1979) The effect of dispersed alumina particle on the electrical conductivity of cuprous chloride, J. Electrochem. Soc. Vol. 126, pp. 1963.
8. Kopp A., Nafe H., Weppner W., Kountouros P. and Schubert H., (1993). Science and Technology of Zticonia V, (eds.) S P S Badwal, M.J. Bannister and R.H.J. Hannink, Technomic Publising Co. Inc. Lancaster.
9. Liang C. C., (1973). U. S. Pat. 3,713, 897.
10. Liang C.C., (1973). Conduction Characteristics of the Lithium

Iodide-Aluminum Oxide Solid Electrolytes, J. Electrochem. Soc.vol.120, pp.1289.

11. Liang C.C., Joshi A. V. and Hamilton N. E., (1978). Solid-state storage batteries, J. Applied Electrochem. Vol. 8, pp. 445.
12. Maier J., (1985). Space charge regions in solid two-phase systems and their conduction contribution—I. Conductance enhancement in the system ionic conductor-'inert' phase and application on AgC1:Al_2O_3 and AgC1:SiO_2, J. Phys. Chem. Solids vol. 46. Pp. 309.
13. Maier J., (1995). Ionic conduction in space charge regions, Prog. Solid St. Chem., vol. 23, pp. 171-263.
14. Nafe H., electroceramics IV, (Vol.II), R. Waser, S. Hoffmann, D. Bonnenberg and Ch. Hoffmann, (eds.), (1994). IWE, RWTH Aachen, University of Technology, Germany, 745-748.
15. Poulsen F. W., Andersen N.H., Kindl B. and Schoonman J., (1983). Properties of LiI-Alumina composite electrolyte, Solid State Ionics, vol. 9&10, 119-122.
16. Rice M. J., Strassler S. and Toombs G. A., (1974). Superionic Conductors: Theory of the Phase Transition to the Cation Disordered State, Phys. Rev. Lett., vol. 32, pp.596.
17. Shahi K. and Wagner J. B. Jr., (1981). Ionic Conductivity and Thermoelectric Power of Pure and Al_2O_3 - Dispersed AgI, J. Electrochem. Soc. Vol. 128(1), pp. 6-13.
18. Singh K. and Bhoga S. S., (1999). SO_x Solid State Gas Sensors: A review, Bulletin of Material Science, Vol. 22, pp. 71.
19. Singh K. and Ratnam J. S., (1988). Electrical conductivity of the Li_2O:B_2O_3 system with V_2O_5, Solid State Ionics vol.31, pp.221.
20. Singh K., (1993). Conductivity mechanism in Li_2SO_4–Ag_2SO_4 binary system, Solid State Ionics vol.66, pp. 5.
21. Wagner Von C, (1956). Zeitschrift Fur Elektrochemie, vol. 60, pp. 4.

Ferroelectrics

ISSN: (Print) (Online) Journal homepage: https://www.tandfonline.com/loi/gfer20

Charge transfer mechanism in $KNbO_3$ dispersed composites of monovalent alkali carbonate

Prashant Ambekar, Jasmirkaur Randhawa & Kamal Singh

To cite this article: Prashant Ambekar, Jasmirkaur Randhawa & Kamal Singh (2022) Charge transfer mechanism in $KNbO_3$ dispersed composites of monovalent alkali carbonate, Ferroelectrics, 587:1, 84-94, DOI: 10.1080/00150193.2022.2034418

To link to this article: https://doi.org/10.1080/00150193.2022.2034418

Published online: 26 Apr 2022.

FERROELECTRICS
2022, VOL. 587, 84–94
https://doi.org/10.1080/00150193.2022.2034418

Taylor & Francis
Taylor & Francis Group

Charge transfer mechanism in $KNbO_3$ dispersed composites of monovalent alkali carbonate

Prashant Ambekar[a], Jasmirkaur Randhawa[b], and Kamal Singh[c]

[a]Dharampeth M. P. Deo Memorial Science College, Nagpur, India; [b]Government College of Engineering, Nagpur, India; [c]Department of Physics, RTM Nagpur University, Nagpur, India

ABSTRACT

The ferroelectric phase $KNbO_3$ dispersed composites of Na_2CO_3 were prepared and studied for its applicability as an electrolyte/sensing electrode in electrochemical sensors. The composites were characterized with *in-situ* impedance measurements under different CO_2 gas partial pressures and transport number measurements. The dispersoid was found modifying the conduction mechanism of ions as revealed from impedance spectroscopy. The electrolyte showed variation in the electrical conductivities in presence of the test gas. Significant improvement in the response time of the electrochemical CO_2 gas sensor was observed while using this composite as an electrolyte cum sensing electrode.

ARTICLE HISTORY
Received 10 January 2021
Accepted 28 December 2021

KEYWORDS
Impedance spectroscopy; $KNbO_3$-ferroelectric phase; electrochemical CO_2 gas sensors; composite electrolyte; monovalent alkali carbonates

1. Introduction

Overwhelming extent of automation in our routine processes has contrived the need of fast, reliable, sensitive, selective and accurate sensors. IOT functioning will also be effective with them when networked for different devices and processes. The state of art developments in CO_2 gas sensors mainly comprise of the following three types viz.

i. Electrochemical sensors (type II or III potentiometric sensor), which are prepared by using pure carbonate components viz. Li_2CO_3, K_2CO_3, Na_2CO_3 are basically hygroscopic nature, develops cracks on thermal cycling, make poor mechanical interface with electrode materials and give sluggish response on reversibility of the device [1].
ii. Semiconducting Metal Oxides (SMO) Gas Sensors comprises of bulk conductivity/surface conductivity variation on CO_2 gas adsorption [2,3]; which have large number of oxide materials for device fabrication but the sensing mechanism need to be clearly understood. Even though the sensing mechanism in SMO sensors is simple, the details of oxygen adsorption (chemisorption) followed by charge transfer processes are complex and further research is required to gather more knowledge of the interaction of CO_2 with SMOs [4].
iii. Perovskite-based Semiconducting CO_2 Sensors are lagging selectivity as they sense different gases simultaneously [5,6].

CONTACT Prashant Ambekar pacific0701@rediffmail.com

The electrochemical potentiometric sensors are best known for following a theoretical relation Nernst law and are selective in nature, which indeed enable them as a long-term solution in the sensor industry. Use of composite materials as electrolyte and/or sensing electrode has been found helping to overcome the above-mentioned shortcomings [7]. For CO_2 gas sensor development, the composite materials can be engineered by addition of insulating phase, ferroelectric phase, glass or glass ceramics to the carbonate host [8].Composite materials are preferred due to high ionic conductivity at lower temperatures and thermal as well as electrical stability in ionic devices [6]. Inert particle dispersed composites have been reported the enhancement of ionic conductivity due to enhanced defect formation at the grain boundary interface. The idea of dispersing ferroelectric instead of inert phase has been thought of by us having vast experience of the ferroelectrics. In this study, in order to achieve enhanced kinetics of ion migration at the grain boundary due to not only inert phase effect but more so due to localized polarization of charges as the ferroelectric phase has permanent dipole moments within the temperature range of device operation. Therefore, $KNbO_3$ phase has been selected for dispersion. Ferroelectric phase having permanent dipole moments results in enhancement of desired properties for sensor application [7]. Sodium ion-based electrolytes are being developed due to low cost of sodium as compared to that of lithium while its chemistry and intercalation kinetics is similar to that of lithium-based materials [9].

A type three sensors using Li^+ ion conducting Li_3PO_4 thin film electrolytes with Li_2CO_3 + Au as sensing electrode has been reported to operate above 460 °C, giving Nernst's slope of −61 mV/decade for the 250–5000 ppm of CO_2 concentration at relatively higher temperature of 500 °C for film thickness 1.2 micrometer [10]. Here, the sensor *emf* is reported to be getting saturated above 5000 ppm. Moreover, as the sensor is using pure Li_2CO_3 it could be used under hygroscopic conditions. This study has reported the failure of thin films (< 300 nm) in development of Nernstian sensors.

Therefore, in order to develop a fast, reliable, durable sensor having usable range and characteristics, in this study, we are presenting an effort to develop a cheap and reliable CO_2 sensor based on the ferroelectric phase $KNbO_3$ dispersed Sodium Carbonate electrolyte. The electrolyte materials are tested using their electrical characterization by *in-situ* Impedance Spectroscopy in different atmospheric conditions and ionic transport number measurement at different temperatures [11]. The material properties will be discussed to find its use as an electrolyte in an electrochemical CO_2 gas sensor.

2. Experimental

The material preparation is an extremely important part of any sensor related research work. The potentiometric sensors are basically having three components, namely, a solid electrolyte, an open reference electrode and a sensing electrode. The schematic of this sensor is shown in Fig. 1, wherein the solid electrolyte is sandwiched between reference and sensing electrodes by proper interface. Of these materials, the electrolyte should have high ionic transference number and the electrodes should have mixed type of conductions within them. Moreover, the contact between electrolyte-electrodes should be proper and there should not be any leakage of gases from the electrolyte to the

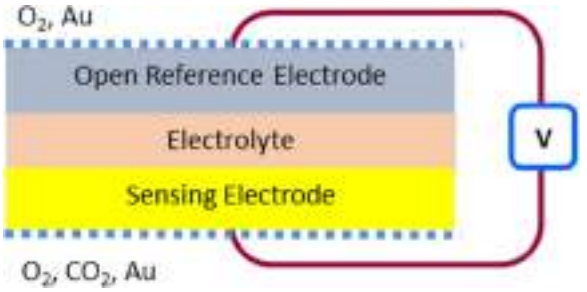

Figure 1. Schematic of electrochemical potentiometric gas sensor.

respective electrodes. Keeping all these factors in mind, materials like $KNbO_3$, composite solid electrolyte and reference electrodes were prepared using conventional melt quenching and/or solid-state sintering techniques. The methods for their preparation are explained below.

2.1. $KNbO_3$ preparation

Well-dried initial ingredients K_2CO_3 and Nb_2O_5 with assay more than 99.5% (procured from Aldrich, USA), were weighed in appropriate mole fraction with an accuracy of 0.01 mg, mixed thoroughly under acetone in an agate mortar for an hour to homogenize the mixture. The mixture was calcified in a platinum crucible over the decomposition temperature 1173 K of the Potassium Carbonate for six hours. The temperature of the mixture was then increased to its melting point 1373 K. The molten material was then quenched in between the revolving twin roller of stainless steel specially made for rapid quenching with a very little gap between them. Thus, obtained material flakes were then pulverized and sieved (400 mesh) to get the fine powder of uniform size for further use.

2.2. Preparation of composite electrolyte

Series of composites of Na_2CO_3 with $>$ 99.5% purity from Aldrich Chemicals, USA having varying weight fraction of $KNbO_3$ (10–80%) were prepared using melt quench technique. The mixture of appropriate weight fractions was treated for melting at about 1125 K for all samples although the melting for few compositions were found far below the said value. The molten mass was soaked in alumina crucible for each composition for about 30 min and then rapidly quenched between clean surfaces of aluminum blocks. The flakes of 1–2 mm thickness were obtained which then crushed-sieved using a 400 mesh for further use. Pellets of diameter 9 mm and thickness ranging from 1–3 mm were formed using a stainless-steel die-punch and a hydraulic press by applying a pressure of 3 tons/cm^2. After sintering them at 823 K for 12 h, the pellets were then used for electrical characterizations applying Pt electrodes at both the surfaces.

2.3. In-situ impedance measurement

All the compositions as discussed in section 2.2 were characterized with impedance measurements in the temperature range from 473 K to 723 K and frequency ranging

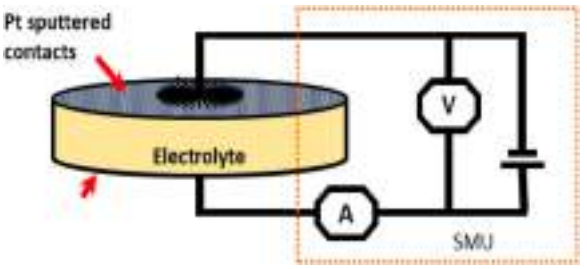

Figure 2. Schematic of experimental arrangement for conducting two probe DC measurements.

from 5 Hz to 13 MHz. The same pellets were then characterized for in-situ impedance measurements under different atmospheric conductions viz. temperatures (473–723 K) and CO_2 concentrations ranging from 0.01 to 100%.The analysis of ac conductivity data has been done manually by plotting impedance plots and Arrhenius plots using MS-Excel and origin software.

2.4. Transport number measurements

The sample composition having maximum ionic conductivity was subjected to transport number measurements using Wagner's dc polarization technique (Fig. 2), for determination of ionic and electronic transport number. The measurements carried out using both blocking electrodes with application of 500 mV for the temperatures ranging from 473 to 773 K in a step of 100 K.

2.4. Sensing characteristics

In order to check the validity of sensing the CO_2 gas in presence of catalyst, same pellets were studied for in-situ electrical conductivity measurements in different CO_2 gas partial pressures in embedded air at elevated temperatures. Also, potentiometric plate type sensor with maximum conducting composite as an electrolyte as well as sensing electrode was fabricated with following cell configuration: Au, O_2, CO_2, Ar/Na_2CO_3 + $KNbO_3$/Na_2SnO_3+SnO_2/Au, O_2, CO_2, Ar. This sensor was tested for response time measurement at 673 K. This sensor being electrochemical potentiometric type, the potential developed at the sensing electrode after test gas adsorption is read by comparing a standard potential of an open reference electrode having same ion for migration. The open reference electrode is made using a bi-phase mixture of Alkali oxide of Rare earths with rare earth oxide in order to achieve the cell reaction as- $SnO_2 + 2Na^+ + 2e^- + 1/2\ O_2 \leftarrow\rightarrow Na_2SnO_3$.

3. Result and discussion

The $KNbO_3$ and its composite with carbonate material were prepared using standardize procedure set-up by one of the authors. The structural characterization confirming the formation of ferroelectric phase and composite nature by structural characterization tools has been discussed in earlier reporting elsewhere [12,13].

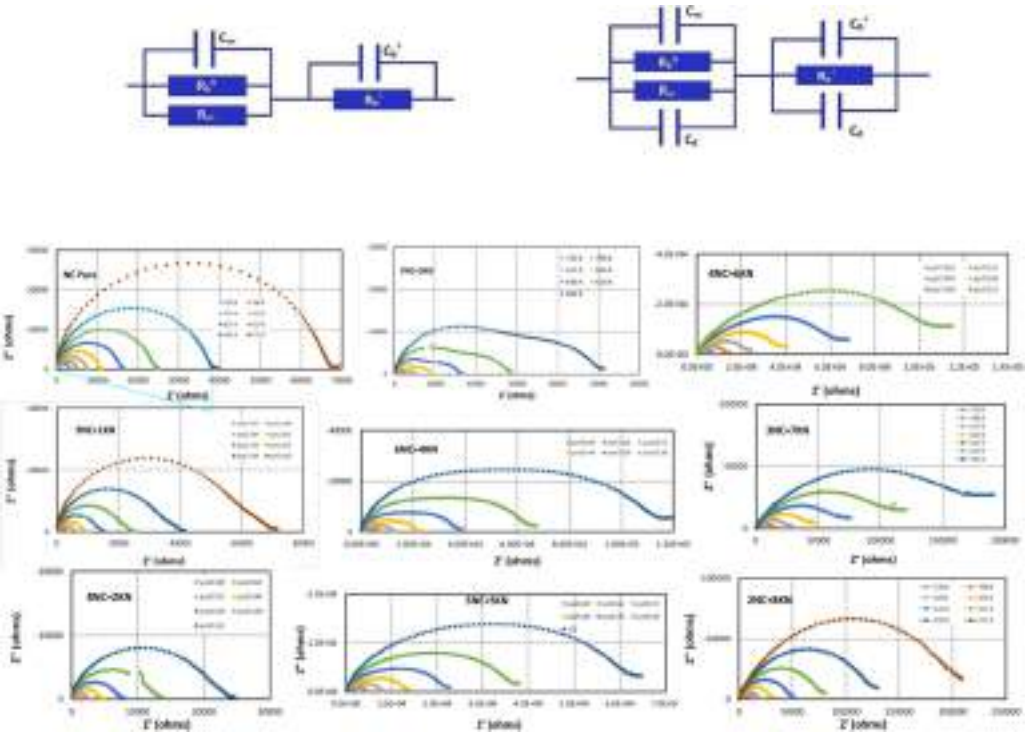

Figure 3. Impedance plots for the binary compositions ranging from 0–80% $KNbO_3$ into Na_2CO_3 at different temperatures.

Figure 3(a) shows the impedance plots for all compositions of the composite electrolyte, depicting two discernible semicircular arcs. The presence of two discernible depressed semicircular arcs is the manifestation of two different conduction regimes within the material [14].The high frequency semicircle corresponds to migration of ions through the bulk of Na_2CO_3 grains as well as parallel to the grain boundaries, whereas the low frequency semicircle suggests migration of ions perpendicular to grain boundaries. These two relaxations are shown by the equivalent circuits in Fig. 3(b). The low frequency semicircle is seen increasing in size with increase in dispersoid $KNbO_3$ concentration.

Complex impedance plots are analyzed by fitting the complex impedance data as per the equation,

$$Z(\alpha) = R_o + \frac{R_{B1}}{1 + (j\omega\tau_1^*)^{a1}} + \frac{R_{B2}}{1 + (j\omega\tau_2^*)^{a2}} \tag{1}$$

Where, R_{B1} and R_{B2} are the bulk resistances related to first and second semicircles (charge transfer mechanisms) respectively; τ^*_1 and τ^*_2 are the mean relaxation times for them [12]. α, an empirical measure of the departure of the charge as learned from the ideal Debye model, is related to the angle of depression ($\theta = \alpha\pi$) of semicircular arc in complex impedance plane. The value of bulk resistance R_B is obtained by taking real axis intercept of the semicircular impedance curve. Bulk resistance was found decreasing with increase in temperature and showed typical composite effect with maximum

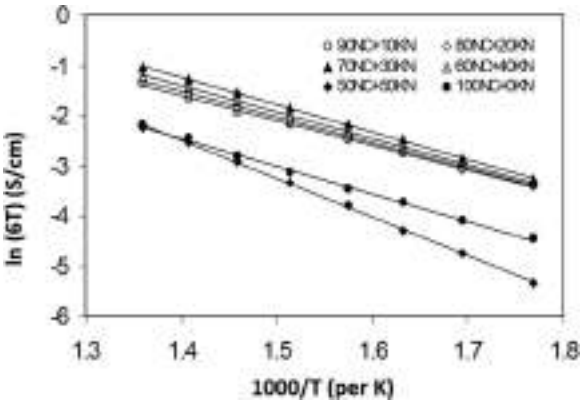

Figure 4. Arrhenius plots for binary electrolyte system (50–100)Na_2CO_3+(50–0)$KNbO_3$.

conductivity at optimum content of inert phase (here $KNbO_3$) in the host [8]. The addition of dispersoid was found modifying the hosts with formation of more than one channels for ionic conduction as revealed from impedance spectroscopy.

Increase in conductivity with higher dispersoid concentration suggest that a greater number of conducting pathways perpendicular to grain boundaries are enabled with increase in dispersoid concentration. Maximum conductivity is observed for the composition $70Na_2CO_3 + 30KNbO_3$, suggesting optimum distribution of dispersoid resulting into connected conduction pathways for ions, which is the typical behavior reported for all inert particle dispersed composites. The equivalent circuit for compositions containing higher dispersoid concentrations is modified with addition of a capacitor C_d in parallel in the low frequency branch [15].

From the Arrhenius plots shown in Figure 4, about one order of magnitude enhancement in conductivity is observed for all compositions having $KNbO_3$ content less than 50 mole%. All compositions have comparable values of activation enthalpy. Though all the four compositions with $KNbO_3$ mole fraction from 10 to 40% gave comparable values of conductivity, the maximum conducting composition $70Na_2CO_3 + 30KNbO_3$ is very clearly identified. Enhancement in conductivity is seen insensitive to composition in low temperature region. For composition $50\,Na_2CO_3 + 50\ KNbO_3$ conductivity is seen decreased for all temperatures with significant drop in at lower temperatures. This decrease in conductivity is also accompanied with increase in activation enthalpy E_a.

Figure 5 shows the plots of relaxation frequencies with temperature for pure Na_2CO_3 and $70Na_2CO_3 + 30KNbO_3$ composite. Activation enthalpy, E_a for the composite electrolyte obtained from the peak frequency values of high frequency semicircles is found comparable with E_a for the pure Na_2CO_3, validating the equivalent circuit. The low frequency data also gives E_a value comparable with pure Na_2CO_3 indicates that the defects created at the interface of Na_2CO_3 crystallite with $KNbO_3$ crystallite are of similar type as that existing in pure Na_2CO_3.

Impedance plots of composite electrolyte $70Na_2CO_3 + 30KNbO_3$ for different CO_2 gas partial pressures at 573 K are seen Fig. 6. Slight decrease in ionic conductivity of the composite electrolyte $70Na_2CO_3 + 30KNbO_3$ is observed with increase in CO_2 gas partial pressure ranging from 0.01 to 10%. This decrease is understood in terms of reduction in Na^+ ions at the electrolyte surface due to its equilibration with CO_3^{2-} molecule

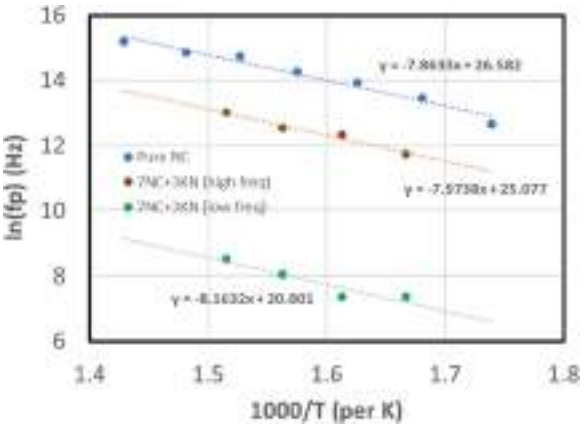

Figure 5. Variation of relaxation frequencies with temperature for pure $Na_2CO_3$and $70Na_2CO_3+ 30KNbO_3$composite.

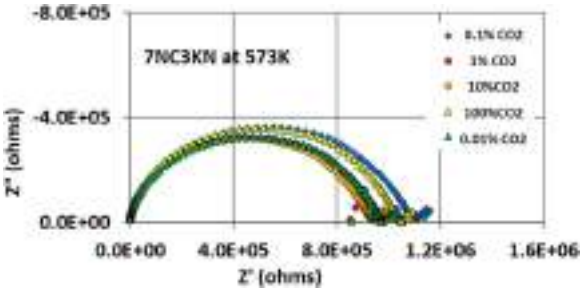

Figure 6. Impedance plots for $70Na_2CO_3+ 30KNbO_3$ binary electrolyte with CO_2 gas partial pressure at 573 K.

creating temporary phase of Na_2CO_3 as $2Na^+ + ½ O_2 + CO_2 + 2e \leftrightarrow Na_2CO_3$. The ionic conduction is found increased for 100% CO_2 gas atmosphere, which is an obvious effect as CO_3^{2-} ions will not be formed in absence of O_2. This is an important parametric effect that needs to be considered in analyzing the sensor characteristics. As per Nernst equation the *emf* of potentiometric CO_2 gas sensor is independent of electrolyte conductivity, but it has been observed that sensors with different electrolyte materials produces different emfs and also their t_{90} response time differs significantly with the electrolytes used.

Comparison of the Arrhenius plots for pure Na_2CO_3 with that of for composite electrolyte can be seen in Fig. 7(A,B). At lower temperatures, the ionic conductivity for pure Na_2CO_3 is found to be significantly affected by CO_2 gas partial pressure variation, the change is being of two orders of magnitudes. At high temperatures the effect of CO_2 atmospheric condition on conductivity is found decreasing (Fig. 7). At high temperature this effect is not significant seen due to increased number of charge carriers giving ionic conductivity.

Arrhenius plots for composite electrolyte of $70Na_2CO_3+30KNbO_3$ shows that the significant variation in conductivity with CO_2 gas partial pressure at low temperatures seen in pure Na_2CO_3 is obviated for its composite with $KNbO_3$. This is due to increased

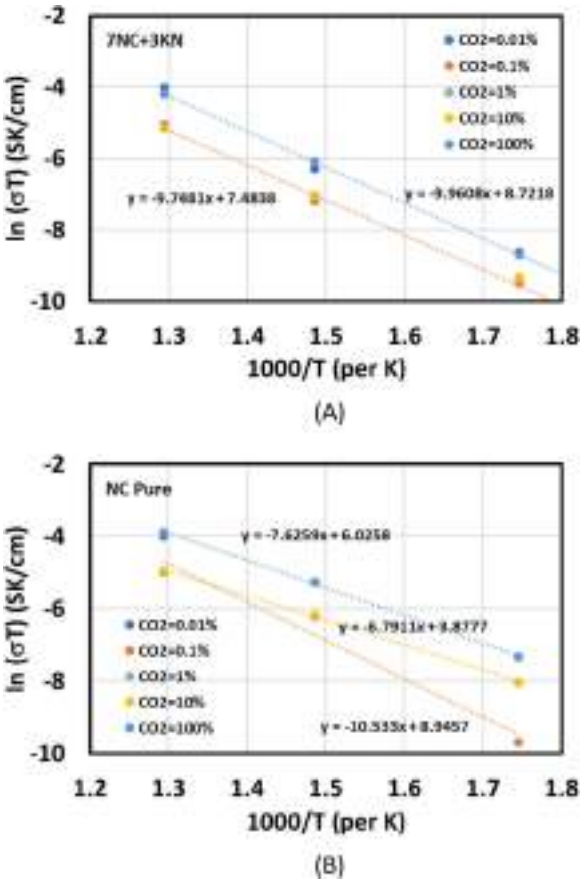

Figure 7. Arrhenius plots for (A) pure Na_2CO_3 and (B) composite electrolyte, $70Na_2CO_3{+}30KNbO_3$ for different CO_2 gas partial pressures.

number of free ions/defects at the grain boundary interface due to surface interactions typically seen in most of the composites [16].

Transport number measurement studies revealed majorly ionic character of the composite $70Na_2CO_3{+}30KNbO_3$, as the sample was getting polarized very fast ($<$ 5 s) with the application of small DC potential through reversible electrodes over a wide temperature range (Fig. 8). A comparison of total conductivity (zero time) σ_0 and electronic conductivity (infinite time) σ_{in} in Fig. 9 shows that the increase in ionic conductivity with temperature contributes to increase in total conductivity, as electronic conductivity is found remaining almost constant. From the values of these conductivities, the ionic and electronic transport numbers are found to be $\boldsymbol{t_i}$ =0.99924 and t_e = 0.00076 at 773 K.

Response of the sensor for toggling CO_2 gas partial pressures between two values 260 and 2600 ppm at 673 K is shown in Fig. 10. The sensor response was found stabilized after 70 min of warm up time. Significant improvement in the sensor response time as well as recovery time of the electrochemical CO_2 gas sensor (i.e. $\boldsymbol{t_{90}}<$ 10 s) was found with this composite simultaneously serving as an electrolyte and sensing electrode. CO_2

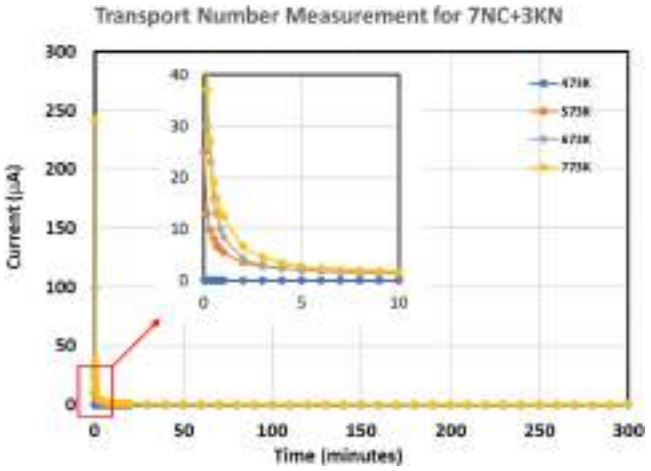

Figure 8. Transport number measurement studies revealed majorly ionic character of the composite $70Na_2CO_3{+}30KNbO_3$.

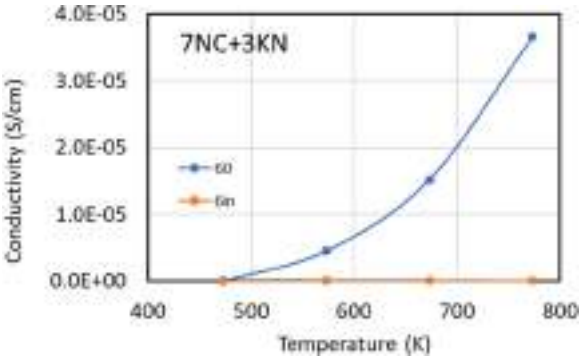

Figure 9. A comparison of total conductivity (zero time) σ_0 and electronic conductivity (infinite time) σ_{in}.

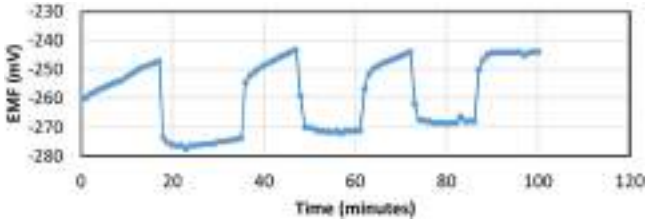

Figure 10. Sensor response for $(Na_2SnO_3)/(70Na_2CO_3{+}30KNbO_3)$ system while CO_2 gas partial pressure toggled between 1 decade of change.

being polar molecule, its adsorption on the sensing surface is facilitated by the charge topography resulting due to presence of ferroelectric phase in the surface. This has resulted in to significant decrease in sensor response time. Enhanced conductivity due to grain boundary effect has provided highly conducting pathways for ion as well as electronic charges. Sensitivity of the sensor was found matching with theoretical value of 28 mV/decade change of P_{CO2} for gas partial pressures range $<$ 785 ppm (Fig. 11).

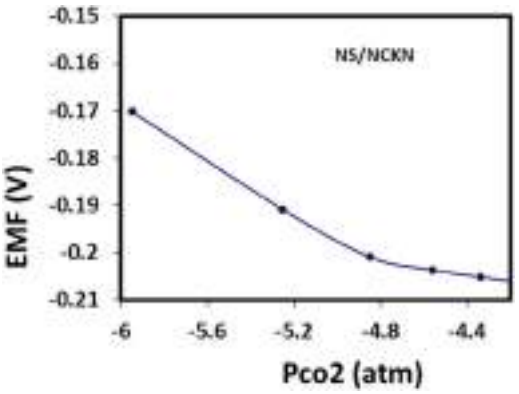

Figure 11. Sensor response for pCO_2 Vs emf developed between sensing ($70Na_2CO_3+30KNbO_3$) and reference electrodes (Na_2SnO_3) while ($70Na_2CO_3+30KNbO_3$) as an electrolyte.

4. Conclusion

The dispersion of hard ferroelectrics into the monovalent carbonates Na_2CO_3 enhances the ion transport perpendicular to the grain boundary as an additional mechanism to that of conduction through the bulk and along the grain boundary. The ferroelectric phase enhances the ionic transport and provides thermal, chemical and mechanical stability to the device. Fast ion migration results in reduced response and recovery times ($t_{90}\sim10$ s) of the sensor which is fastest among all composite as well as binary electrolytes.

Funding

Authors are thankful to CSIR, New Delhi; UGC WRO, Pune; IAS Bangalore for providing partial financial support to carry out this work.

References

[1] P. Ambekar, J. Randhawa, and K. Singh, Stabilizing the sensing electrode kinetics of an electrochemical co$_2$ gas sensor using materials engineering, *Adv. Sci. Lett.* **20** (3), 565 (2014). DOI: 10.1166/asl.2014.5387.

[2] G. Lamdhade, Tin oxide and titanium dioxide based co 2 gas sensor, *J. Electron Dev.* **21**, 1849 (2015).

[3] P. Samarasekara *et al.*, CO_2 gas sensitivity of sputtered zinc oxide thin films, *Bull. Mater. Sci.* **30** (2), 113 (2007). DOI: 10.1007/s12034-007-0020-y.

[4] S. Mulmi, and V. Thangadurai, Electrochemical carbon dioxide sensors: Fundamentals, materials and applications, *J. Electrochem. Soc.* **167** (3), 037567 (2020). DOI: 10.1149/1945-7111/ab67a9.

[5] F. Jeffrey, Perovskite oxides for semiconductor-based gas sensors, *Sens Actuators B Chem.* **123**, 1169 (2007).

[6] J. Randhawa *et al.*, $AgNbO_3$ dispersed Ag_2SO_4 composite for potentiometric SO_2 gas sensor application, *Ionics* **10** (1-2), 39 (2004). DOI: 10.1007/BF02410303.

[7] P. Ambekar, J. Randhawa, and K. Singh, Modified transport properties of $LiNbO_3$ dispersed Li_2CO_3 composite system for electrochemical CO_2 sensor, *Adv. Mater. Lett.* **5** (2), 75 (2014). DOI: 10.5185/amlett.2013.fdm.20.

[8] C. Liang, U.S. Pat.3,713 (1973), 897.
[9] J. Aniruddha, P. Rajib, and R. Ajit, Chapter 2 - Architectural design and promises of carbon materials for energy conversion and storage: in laboratory and industry, in *Carbon Based Nanomaterials for Advanced Thermal and Electrochemical Energy Storage and Conversion, Micro and Nano Technologies* (Elsevier, Amsterdam, 2019), 25 p. DOI: 10.1016/B978-0-12-814083-3.00002-0.
[10] L. Satyanarayana, S. Park, and W. Noh, Potentiometric CO_2 sensor using Li + ion conducting Li_3PO_4 thin film electrolyte, *Sensors* **5** (11), 465 (2005). DOI: 10.3390/s5110465.
[11] V. Wagner, Zeitschrift fur elektrochemieberichte der bu nsengesellschaft fur physikalischechemie, *Zeitschrift Fur Elektrochemie* **60**, 1 (1956).
[12] K. Singh, P. Ambekar, and S. Bhoga, Investigation of Na_2CO_3-ABO_3 (A = Li/K/Ba and B = Nb/Ti) heterogeneous solid electrolyte systems for electrochemical CO_2 gas sensor application, *Solid State Ion.* **122** (1-4), 191 (1999). DOI: 10.1016/S0167-2738(99)00033-8.
[13] S. S. Bhoga and K. Singh, Li_2CO_3 –ABO_3 (A = Li, K, Ba and B = Nb, Ti) composite solid electrolyte systems, *Solid State Ion.* **111** (1-2), 85 (1998). DOI: 10.1016/S0167-2738(98)00160-X.
[14] J. Maier, Defect chemistry in heterogeneous systems, *Solid State Ion* **75**, 139 (1995). DOI: 10.1016/0167-2738(94)00222-E.
[15] B. Sundarakannan, K. Kakimoto, and H. Ohsato, Frequency and temperature dependent dielectric and conductivity behviour of KNbO3 ceramics, *J. Appl. Phys.* **94** (8), 5182 (2003). DOI: 10.1063/1.1610260.
[16] K. Hariharan and J. Maier, Enhancement of the fluoride vacancy conduction in $PbF_2 : SiO_2$ and $PbF_2 : Al_2O_3$ composites, *J. Electrochem. Soc.* **142** (10), 3469 (1995). DOI: 10.1149/1.2050006.

International Journal of English Literature and Social Sciences
Vol-6, Issue-4; Jul-Aug, 2021

Journal Home Page Available: https://ijels.com/
Journal DOI: 10.22161/ijels

Peer-Reviewed Journal

Investigation of the Role of Goal Setting Objectives and its Outcomes among Young Learners

Dr. Mrs. Shraddha. A. Deshpande

Assistant Professor and Head, Department of English, Dharampeth M. P. Deo Memorial Science College, Nagpur, India

Received: 03 Jun 2021; Received in revised form: 25 Jun 2021; Accepted: 02 Jul 2021; Available online: 9 Jul Jun 2021

Abstract— *Focus and direction are the primary aspects of teaching and learning when you are dealing with young learners. The age demands it; however it is observed that it is the least important task they are persuaded to. Any task of learning requires well-defined steps of goal setting that eventually transcending them to their accomplishments. At the same time, consistent efforts in the direction of their set goals are the keys to their actual success of learning. When given a choice of attempting a particular task, like joining a Language and a Literature Club, it was observed that more than average number of learners had specific goals in being a part of each clubs. The present paper aims at studying the goal setting objectives of the young learners towards the learning process. It also presents the contributions of the learners thatwere instrumental in achieving their well-defined personal and profession goals. The study is based on Edward Locke's Goal Setting Theory which postulates that people work better and harder and are motivated when they are inclined to achieve a particular target.*

Keywords— ***Edward Locke's Goal Setting Theory, Five Principles of Goal Setting, Online Learning, moral developmental milestones for adolescents.***

I. INTRODUCTION

Motivation is the key for task completion, then be it for employees or students. Employees need to perform to raise their incentives whereas the students need it to get that job. Therefore in order to achieve these desirable goals, one has to involve in proper planning and clear goal setting initiatives. It was in the year 1960s Edwin Locke postulated the Goal-setting theory of motivation, which emphasises on study of the impact of specific and challenging goals established on the task performance feedback. The study is essentially employee focused; nevertheless, it can also be attuned to learners involved in learning a specific task of their choice. The very core aspect of Locke's Goal Setting Theory is based on five principles of Goals and its subsequent performance that involves Clarity, Challenge, Commitment, Feedback, and Complexity. His well-researched published paper called Toward a Theory of Task Motivation and Incentive in 1968, impressed Dr. Gary Latham, who collaborated with him in producing A Theory of Goal Setting & Task Performance, a book that expanded the theory.According to Locke and Latham, there are five goal-setting principles that can increase the chance of success:

- **Clarity:** Goals should be SMART
- **Challenge:** Goals should be challenges that care within the reach of the performer, neither too easy nor too difficult.
- **Commitment:** Goals should have self-motivation for achieving desired outcomes.
- **Feedback:** Consistent check on whether the set goals are heading in the right direction or not.
- **Complexity:** Goals if seemed complex can be redesigned by modifying allotted time and other needful criteria.

Locke's Goal Setting Theory in Educational Context:

The objectives of any learning are always well defined, time bound and focused on specific outcomes. The learners are expected to go through the syllabus in order to

decide whether to opt for the specific learning. However, learners are not always aware of their judgment as to why they have chosen a specific course. Eventually the coursework as well as the teaching-learning process becomes an ambiguous experience for them, further declining them interest interest in the topic. Their cognitive ability weakens and learning stops. In some cases, the learners continue learning in the same manner and superficially succeed by attaining required scores and proceed with a degree. But the outcome remains the same, in reality, the learning has never occurred. In other few cases, a new course is chosen with the same approach and the journey of failure continues. Nevertheless, few of them who decide to study, understand analyses, and evaluate the process of choosing a well-defined goal, surely receive their outcome. They either refer to or are aligned to the concept of SMART goals, first written down by, "George T. Doran, a consultant and former Director of Corporate Planning for Washington Water Power Company. He in his paper, Doran provides some clarification for readers on applying the SMART acronym:

'How do you write meaningful objectives?'- that is, frame a statement of results to be achieved, Managers are confused by all the verbal from seminars, books, magazines, consultants, and so on. Let me suggest, therefore, that when it comes to writing effective objectives, corporate officers, managers, and supervisors just have to think of the acronym SMART. Ideally speaking, each corporate, department, and section objective should be: (SMART). [1]

Long before that, in 1968, Edwin A. Locke has postulated that workplace management can produce motivation that improves performance and allures incentives. He in his, ground-breaking Goal Setting Theory in collaboration with Dr. Gary Latham suggested five principles, and two main characteristics that focused not only on the primary process of goal setting but also on the efforts required to put for expected outcomes. As one can see, how the application of SMART goals have helped people from different corporate and management field to achieve their targets, the same application can also be utilized for setting goals at academic level for young learners.

The objective of the study:

- To investigate whether learners set goals before they decide to participate in a learning activity of their choice.
- To investigate how learners perform to their set goals regarding any learning activity of their choice.
-

Assumptions:

- Learners set goals while choosing an activity of their choice.
- Learners perform better when they have set goals to participate in the activity of their choice.

II. RESEARCH METHODOLOGY

The research was performed in the form of an experiment to determine the decision-making capacity of adolescents to participate in a specific learning activity in the backdrop of boredom and inactivity the pandemic has created for them for more than one. An English Language Learning Club and An English Literature Club have been formed on Whatsapp and around students of Bachelor of Science of all the three years joined the groups in gusto. English Junction

This group was based on teaching the English Language that focused on teaching English from basics.

- 113 students initially joined the group and the teaching initiated with the nouns, verbs, adverbs, adjectives, and so on.
- Text and Visuals were used to explain the basic concept.
- Online discussion was carried out simultaneously to solve more examples and queries.

Outcome:

Students learned grammar and participated in solving exercises. 35 students out of 113 were active in the group. The remaining students were removed from the group. With consistent requests to re-join, the total number raised to 43.

English Literature Gateway

The next activity was introduced as a learning platform for English Literature.

- 54 members joined the group and were consistent in their performance.

Outcome: Students wrote their own quotes, shared poems of their choice, and wrote poems based on the video shared with them. 54 students actively participated in all the writing and reading tasks assigned to them in the stipulated time.

Findings:

Clarity:

- 64.9% of the learners agreed that they had specific goals in joining this group, remaining were unsure of it.
- Out of them 89.2 were self-motivated and 10.8% did not think so.

- Purpose of joining was, 64.9% had interest, 24.3% had a passion and 10.8% had liked to join the learning activity.
- Their goals for joining this group was to learn about English Language and Literature and (51.4%), Develop Creative Writing Skills (62.2%), Enjoy Language and Literature (21.6%), for professional Development (59.5%), personal development (35.1%)

Challenges:

- 47.1% voted that they cannot write like others, 38.2% cannot write every day.
- 71.1% learners felt joining this group has motivated them, 14.3% felt had enhanced them as an artists, nevertheless, 8.6% demoralised them for their lack of creativity.

Commitment:

- 73% wanted to stay because they are learning,
- The learners were committed to staying in the group, participate in team activities (69.4%) ask questions to raise knowledge (19.4%), reading at least once in 2 days (11.1%).
- Their commitment enhanced in the group by 44.4% if they are appreciated and motivated for their contribution, provided with new knowledge, 36.1% if they get the opportunity to collaborate.

Feedback:

- Feedback on the content given by the learners is as 43.2% felt it was knowledgeable and appropriate, 29.7% felt it was relevant and interesting, 27% voted it to be informative and creative.
- Feedback on teaching style was 56.8% interesting, 24.3% understandable and 13.5% appropriate.
- Feedback on the pace of the class: 83.3% appropriate, 8.3% for slow and fast.
- Feedback on peers: 77.8% creative, 61.1% competent, 27.8% collaborative, 11.1%attidunious, 2.8% incompetent.
- Feedback of feedback given by the teachers, 77.8% were of the opinion it was regular, 13.9% intermittent, and 8.3% irregular.

Task Complexity:

- 82.5% of learners said that tasks were matching their goals, 10%behind their goals, and 7.5% ahead of their goals.
- Out of the 52.5% are achieving the deadlines and remaining, just reaching it.
- For 75% of them the assignments are appropriate, for 17. % they are easy and for rest, they seemed complex.
- The last and important question was: What if the tasks become complex in the progression of the learning? To which, 67.5% responded that they will try to learn, and the remaining would enjoy the challenges of the complex task.

III. CONCLUSION

The search for knowledge is a difficult task, FabiolaGianotti opined, but what to search and why to search are its pre-requisites. It is imperative to understand the purpose behind initiating a task and then also equally important is its execution. A well-defined task can procure the most expected results. The learners in the above experiment had specific objectives in their mind before joining the activity; therefore the results they got were extremely satisfactory and fruitful. The outcomes were measurable and enjoyable in the form of the creative writings of the learners. The discussions were deep and extensive, till the learning was not accomplished. Few learners were apprehensive about their participation, but self-paced learning helped them to overcome this issue as well. Also, the consistent attendance in the group was monitored that maintained the gravity of the teaching-learning process. This approach created a sense of responsibility towards the progression of their pre-defined goals. The learners had done exactly what Tony Robbins had said' "Setting goals is the first step in turning the invisible into the visible.

IV. RECOMMENDATIONS

One of the major aspects of the National Education policy is the introduction of a multidisciplinary College in every district which emphasizes the flexibility offered to students to choose their choice of subjects. This kind of freedom gives learners a chance to critically think, self-analyse, and then commit to a particular career based on their own liking and capability. The whole process will involve a goal-setting initiative as a vital step for these inspiring aspirants, to begin with. Such a pragmatic start will ensure their smooth and encouraging academic journey which was otherwise burdened by the gamut of compulsory subjects. However one cannot go away with the problems

of compulsory subjects in the present education system. In some cases, we can introduce a liberal approach by offering learners such activities they can enrol by choice. English Language Junction and English Literature Gateway were such platforms offered to the students of Language and Literature Learning. As the learners chose to be a part of these groups on their own, they were most benefitted, as rightly quoted by Jean-Paul Sartre "We are our choices."

REFERENCES

[1] Dotson, R. (2015). Does goal setting with elementary students impact reading growth? (Doctoral dissertation). Retrieved from ProQuest Dissertations Publishing. (Accession No. 10019493).

[2] Doran. (1981). There's a S.M.A.R.T. way to write management's goals and objectives. Management Review, 70(11), 35-36.

[3] Hwang, Y. (1995). Student apathy, lack of self-responsibility and false self-esteem are failing American schools. Education, 115(4), 484-490.

[4] Jenkins, D. (1994). An eight-step plan for teaching responsibility. The Clearing House: A Journal of Educational Strategies, Issues and Ideas, 67(5), 269-270.

[5] Smith, E (2007). Considering the experiences of 'underachieving' and 'overachieving' student'. International Journal of Research and Method in Education. 30(1), 19-32. doi: 10.1080/17437270701207702

[6] Smith, E. (2003). 'Understanding under achievement: an investigation into the differential achievement of secondary school pupils'. British Journal of Sociology. 24(5), 575-586. doi: 10.1080/0142569032000127143.

[7] https://www.projectsmart.co.uk/brief-history-of-smart-goals.php

[8] https://peakon.com/blog/employee-success/edwin-locke-goal-setting-theory/

[9] https://getlucidity.com/strategy-resources/guide-to-locke-s-goal-setting-theory/

I J R B A T, Issue (X) Vol (II) May 2022: 316-323

A Double-Blind Peer Reviewed & Refereed Journal

OPEN ACCESS

e-ISSN 2347 – 517X

Original Article

INTERNATIONAL JOURNAL OF RESEARCHES IN BIOSCIENCES, AGRICULTURE AND TECHNOLOGY

 www.ijrbat.in

SWOT ANALYSIS OF CLEAN FUEL PROGRAMME INITIATIVE IN INDIA

Dr. Vaishali Jaiswal[1], Dr. Vaishali Meshram[2] and Dr. Pravin Meshram[3]

[1]Assistant Research Officer, Dept of Epidemiology,
NIHFW, Munirka,New Delhi

[2]Head, Dept of Chemistry,
Dharampeth M.P.Deo Memorial Science College,Nagpur

[3]Professor & Head, Dept of Environmental Science,
Sevadal Mahila Mahavidyalaya, Sakkardara Square, Nagpur

Communicated :27.03.2022 | Revision : 05.04.2022 Accepted :10.04.2022 | Published: 02.05.2022

ABSTRACT: Cooking is an important aspect to human lives. A sizable portion of India's population still relies on biomass fuels, such as wood, animal wastes, and agricultural residues, to meet their energy needs for cooking. According to the 2011 census, 67.3% of the Indian population used biomass fuel for cooking. Also, the cooking devices used had poor thermal efficiency and posed a severe threat to health due to unclean combustion. Clean cooking fuels are a highly cost-effective health intervention and household's energy-behavior indicates the economic development of a country .The past few decades have seen immense efforts by the Indian Government to introduce improved cookstoves and other cleaner cooking fuels; however, most of these interventions have largely failed to bring the much-needed transition. Learning from past experiences, the Government of India initiated the National Biomass Cookstoves Initiative(NBCI) in the year 2009. This program uses a different approach based on the changes that have taken place in society and technology over the years. In "Pradhan Mantri Ujjwala Yojana" (PMUY), the government provided gas connections to a total of 50 million poor households (from 2016 to 2018) .Piped Natural Gas (PNG) connections have reached more than 11% of households annually with a goal of 20 million by early next decade helping to move LPG to rural areas. In the present paper, Strengths, Weaknesses, Opportunities, and Threats (SWOT) analysis has been done on clean cooking programs to determine the extent to which the new program is likely to ensure access to clean cooking energy for all.

Key words: - Biomass fuel, National Biomass Cookstove Initiative, PMUY, Improved Cookstove, SWOT, India.

INTRODUCTION :

Household air pollution is recognized as a significant source of potential health risks to exposed populations throughout the world. The major sources of household air pollution worldwide include combustion of fuels, tobacco smoke, ventilation systems, furnishings, and construction materials. These sources vary considerably between developing and developed nations. Worldwide most research into and control of indoor air pollution has focused on sources of particular concern in developed countries, such as Environmental Tobacco Smoke, volatile organic compounds from furnishings and radon from Soil [1]. The most significant issue that concerns indoor air quality in household environments of developing countries is the exposure to pollutants released during combustion of solid fuels, including biomass (wood, dung, and crop residues) or coal used for cooking and heating.

Nearly half the world continues to cook with solid fuels such as dung, wood, agricultural residues and coal. In India, approximately 86.7% of rural households and 26.3% of urban households rely on solid biomass fuels for their cooking needs [2] .This practice can adversely impact respiratory health of individuals and local forests and other environmental resources, as well as contribute to climate change [3–8]. When used in simple cooking stoves (mostly traditional Indian Chulah), these fuels emit

substantial amount of toxic pollutants that include respirable particles, carbon monoxide, oxides of nitrogen and sulfur, benzene, formaldehyde, 1- 3-butadiene, and poly aromatic compounds, such as benzo (α) pyrene [9]. In households with limited ventilation as is common in rural household of developing countries, exposures experienced by household members, particularly women and young children who spend a large proportion of their time indoors, have been measured to be many times higher than World Health Organization (WHO) guidelines [10].According to WHO[11] indoor smoke from solid fuels ranked as one of the top ten risk factors for the global burden of disease, accounting for 4.3 million premature deaths each year. Household air pollution (HAP) arising from combustion of solid fuels for cooking is a major contributor to four of the top five causes of mortality and morbidity in India, and HAP is also a significant contributor to outdoor air pollution[12,13,14].

In India, the most commonly used stove for cooking is the traditional mud stove called a 'Chulha' which has been adapted to burn all kinds of biomass fuels. When the solid biomass fuels are burnt in such stove, a major fraction of the fuel's available energy goes waste because of its low efficiency. Another problem associated with these cooking devices is their inability to vent smoke out of kitchen, which results in smoke being trapped in kitchen leading to building-up of indoor pollution levels that are high enough to cause serious health problems [15]. In context of the above cited concerns, to design and develop the most efficient, cost effective, durable and easy-to- use cooking device in India, the Department of Non-conventional Energy Sources (DNES), had initiated demonstration of improved cookstoves soon after its inception in 1982, followed by the launch of National Program on Improved Chulhas (NPIC) in 1983 which ended in 2004 (16). The program had two primary aims, first to reduce demand on fuel wood to check widespread deforestation; and second, to improve health by removing smoke from kitchens. The program aimed to disseminate improved cookstoves in the community. A total of 33.8 million improved cookstoves were installed under this program with varying degree of success in different regions of the country. Some models had better acceptability than others in specific regions. Some states such as Haryana, Maharashtra and West Bengal of the country showed greater enthusiasm on the part of the users to adopt new designs [17]. For a variety of reasons, the program brought a mixed bag of experiences [18,19]. In 1992, the DNES was upgraded as the Ministry of Non-conventional Energy Sources (MNES) and continued to manage this program. In 2009, the ministry was renamed as Ministry of New and Renewable Resources (MNRE). The context of concerns over health, climate change and energy security, the Ministry of New and Renewable Energy (MNRE), Government of India launched National Biomass Cookstoves Initiative (NBCI) in December 2009 with the primary aim to increase the use of improved biomass cookstoves [20]. The initiative stressed upon setting up of state-of-the-art testing, certification, monitoring facilities and strengthening research & development (R&D) programs. Although there are far better biomass cookstoves than in the past, they have not progressed to the point that they are equivalent to gas in terms of reliability, flexibility, durability, efficiency, and cleanliness. Confirmatory evidence is that few, if any, women who have the option will change from gas to biomass, but many tens of millions do the reverse every year when given the chance. New biomass stoves are still coming, however, and we can hope that some will perform well enough over time in village households to be true competitors[21].

Recent research suggests that providing clean cooking fuels to all can be a highly cost-effective health intervention [22]. In addition, collection and use of solid fuels for cooking increases the drudgery and adversely impacts time use by women [23,24]. To promote clean cooking fuels in 2015, Government of India and the 3 oil marketing companies that market LPG in India started three major programs to actively promote LPG to the poor , each pioneering, and relying heavily on both sophisticated social marketing and(JAM) electronic bank accounts, biometric ID cards, and mobile phones. The first program, Pahal, shifted to paying subsidy fuel payments into people's bank accounts and thus all LPG is now sold at international rates in the market, greatly reducing diversion of LPG to the non-household sector. The second, "Give it Up", persuaded middle-class households to give up their subsidies to connect the poor. The third, Pradhan Mantri Ujjwala yojana (PMUY) which is underway now, will provide connections to a total of 50 million poor households by 2019 and has reached 20 million already by April 2017.In addition, although starting from a small base, PNG connections have been growing at more than 11% annually with a goal of 20 million by early next decade [25]. Each of these frees up LPG to be moved to rural areas and reduces the LPG import burden.

Since the NBCI has completed 12 years and PMUY more than 5 years , it is worthwhile to assess the program using the analysis of strengths, weaknesses, opportunities and threats (SWOT) to draw an analytical profile. This would help identify gaps and threats in the program so that the same could be utilized to improve the program's performance throughout the country

Strength

- **Multiple stakeholders**

There are many actors in the household energy sector in India. They include governmental agencies, oil marketing companies that market LPG ,Non-Government Organizations (NGOs), research institutes, multinational organizations, donor agencies, etc. NBCI is being implemented through R&D/academic institutions .Besides this, the State Nodal/Implementing Agencies, State Departments of Education through District Coordinators of MDM Scheme, District Level Officers of Anganwadis, District Coordinators/Officers of Tribal/Scheduled /Backward Caste Hostels and similar departmental agencies where cookstoves could be employed. Also, the NGOs, manufacturers, business development organizations, etc. engaged in the implementation of renewable energy projects at the grass-root level are part of the program.

Huge market potential for clean fuel

Despite rapid urbanization, about 70% of Indians still reside in rural areas. Most villagers still depend predominantly on traditional fuels to meet their energy needs. The use of biomass fuels like wood, dung cake, and crop residue is widespread in rural areas. According to the 2001census, 74% of Indian households relied on biomass as their primary cooking fuel, which has come down to 67 % according to the latest Census conducted in 2011 . So, the target population is still above 50% of Indian households.

- **Multiple Choice of Clean Fuels**

GOI promotes many clean fuels to give the users a basket of choices from which they can pick the stove that meets their needs the best in terms of the variety of cooking practices, fuels, and levels of affordability.

Both engineering and non-engineering parameters are now taken into consideration in designing appropriately improved cookstoves. The majority of cookstoves in the market are tailored to provide a more advantageous cooking

experience without requiring any fundamental change in user cooking habits

- **Indirect benefits of Clean Fuels**

The use of solid biomass fuels for cooking is the largest source of HAP in India, particularly in rural areas where more than 85% of the households still depend on biomass for their daily cooking needs. It is now widely recognized that improved energy services at the household level can reduce child mortality rates, improve maternal health. It reduces the time and the transport burden on women and young girls for cooking and fuel collection to have more time for education and other productive works[26]. It is also recognized now that effective household energy programs can lessen the pressure on fragile ecosystems [27].

- **Issues of Cookstove safety**

In the new designs of cookstoves, precautions have been taken against sparks and burns. Equal importance is given to stability against tilting while stirring the food during cooking, especially in the portable stoves. Therefore, the new, improved cookstoves are safer as compared to the previous models.

Opportunity for employment generation at the local level

Involving the local community in various operational aspects of the cookstoves in the new program offers immense possibilities for their participation and entrepreneurship in the program, especially for women through self-help groups. The community gets a sense of ownership as they are involved in various aspects of the program

Weakness

- **Lack of Awareness**

Research suggests that rural people are not concerned about cooking fuels and deforestation issues, mainly due to a lack of awareness. Householders are often unaware of the detrimental health and environmental effects of smoke from traditional cooking practices. Therefore, they lack the knowledge of the health benefits from improved cooking stoves, especially to women and children. Recently, a pilot study conducted in three Indian states reported that only 14% of households believed that adopting a clean stove could alleviate the adverse health effects of traditional cooking.

- **Socio-Cultural Factors**

Despite changes in the program, certain strong cultural factors prevent widespread use of efficient cookstoves. They include traditional cooking practices, and other benefits such as space heating by conventional cookstoves, and slow cooking when the women are out in the fields. It is essential to ensure that the improved cookstoves allow women to continue with their traditional cooking practices. The current program may not be able to overcome these forces Multiple stakeholders While many levels of stakeholders are seen as strengths to the program, they also make the program's administration cumbersome and fragmented. Coordination with all the concerned stakeholders is a challenging task for the implementing agency.

- **Financial implications**

Although improved stoves save money in the long run, the initial investment required for a really clean stove may prevent poor people from purchasing it. Where communities were required to pay the full cost of the improved cookstoves, the price was reported as an important barrier among poorer households [28] [Sesan, T.A., 2012.]. In the pilot study conducted in three states of India, the majority (63%) of randomly selected households cited cost as the least desirable aspect of the improved cookstoves[29] [Jessica, J.,et.al 2015]. Although consumers are willing to adopt new cooking approaches, the product must be cost-competitive with existing solutions such as LPG stoves [30]

- **Slow switch-over to cleaner fuels**

As income increase, households generally switch-over to cleaner and more efficient fuels for their domestic energy needs, i.e., move up the 'energy ladder.' However, in many rural areas, households often employ 'multiple models' of stove and energy use, and fuel substitution is often partial. As a result, the full benefits of "clean" stoves are not achieved. As per the 2001 census of India, biomass fuel use in households was nearly 74%, which came down to 67% in the 2011 census. [Census, 2001 &2011] While conversion to modern fuels has accelerated in urban areas, populations in rural areas have remained slow in moving away from solid fuels.

Opportunities

- **Huge market potential**

As income increase, households generally switch-over to cleaner and more efficient fuels for their domestic energy needs, i.e., move up the 'energy ladder.' However, in many rural areas, households often employ 'multiple models' of stove and energy use, and fuel substitution is often partial[31] . As a result, the full benefits of "clean" stoves are not achieved. As per the 2001 census of India, biomass fuel use in households was nearly 74%, which came down to 67% in the 2011 census. [Census, 2001 &2011] While conversion to modern fuels has accelerated in urban areas, populations in rural areas have remained slow in moving away from solid fuels. It can act as a roadblock in the successful implementation of the program.

- **Opportunities for public-private partnership**

The clean fuel Initiative opens up opportunities for applying the public, private partnership (PPP) model at all levels. If such alliances are implemented effectively, it can provide an opportunity for all stakeholders such as Government, industry, academic institutions, and social sector to benefit from each other's expertise and resources. Micro-institutions such as NGOs, creditors, and retailers can also be vital for delivering improved cookstoves in India

- **Raised public awareness**

There is an increased awareness of air pollution and its health impact in India due to epidemiological research and greater media exposure. Therefore, there is a widely felt need for providing cleaner cooking options to improve household air quality in rural households at an affordable price.

Threats

- **Slow progress of the program**

Better from the earlier program, yet the development of the programs has remained slow so far. The country's NBCI's Initiative seeks to provide nearly 166 million improved cookstoves to households currently using solid biomass fuel, which was too ambitious). Though the overall cookstove market size in India is vast, the easiest consumer segment to target would be mid and high-income biomass fuel users. A big challenge would be rural biomass fuel users who could make up about 85% of the market as they do not have a habit of paying for fuel (as biomass is freely available in rural areas.

PMUY did not scale-up in the Maharashtra as, the number of connections given in the whole Nagpur district till 2018 was only 12,000 [33]. So, considering that Nagpur has 14 blocks, these numbers are less as compare to other parts of India. The findings also show widespread fuel stacking as shown by the works of other researchers . As a result, the full benefits of clean fuels are not achieved. Conversion to cleaner fuels in study areas has remained slow because the cost of fuel is the limiting factor[34]. For the BPL population to shell out Rs 700 per month is a big deal as they don't get the subsidy. Many villagers find gas too costly as 43.9% of the population uses biomass as it is freely available and in any case, they have to burn it. The result corresponds to similar

findings from the PMUY study done by Ahmad N and a clean cooking alliance study in Karnataka

- **Inadequate coordination among key players**

Cookstoves have become a popular focus area for donor agencies on financing and supporting research. Still, the Government needs to ensure that the program's objectives may not get diluted due to the pressure of multiple agencies. Sometimes, administrative arrangements and the donor partner's requirements may work against market sustainability .In particular, short-term projects may not focus on sustainable use of improved technologies. This lack of proper coordination among donors, program coordinates, and stove users emerged as a barrier to creating sustainable change

- **Role clarity of different stakeholders**

As the program has multiple stakeholders, each stakeholder's roles and responsibilities must be clarified right in the beginning else; it would result in overlapping of work or missing some critical aspect altogether. Effective strategies to reduce the burden of HAP require commitments from various sectors. Though different ministries (e.g., health, environment, rural development, MNRE, housing, poverty alleviation, oil and natural gas, women and child development) aim to

CONCLUSION:

To address the HAP, the last few decades have witnessed many household energy initiatives taken by the Government of India. Still, the pace of switching over to clean fuel/stove has not been very encouraging. The SWOT analysis of the clean fuel program suggests that it contains several promising elements as it has incorporated the concerns raised in the previous programs. The lessons learned from earlier experiences can be the guiding force in implementing a successful household energy program. The present program has some limitations too. Therefore, the GOI and the implementing ministry needs to develop its strategies to capitalize upon the program's strengths and opportunities and draw up action plans to minimize its weaknesses and threats. If appropriately implemented, the program can ensure access to clean and sustainable cooking energy in India.

REFERENCES:

Spengler JD, Sament JM, Mccarthy F (2001) Indoor air quality handbook, Mccraw Hill New York

Census of India, 2011. 'Houses, Household Amenities and Assets', Government of India. Retrieved 05/09/2017 from http://www.devinfolive.info/censusinfo dashboard/website/index.php/pages/kitchen_fuelused/Total/insidehouse/IND

Behrens A, Lahn G, Dreblow E, Nuñez-Ferrer J, Carraro M, Veit S. Escaping the vicious cycle of poverty: Towards universal access to energy in developing countries. Brussels:Centre for European Policy Studies; 2012. CEPS Working Document 363.

Barnes DF, Floor WM. Rural energy in developing countries: a challenge for economic development. Annu Rev Energ Environ 1996;21:497-530.21

Ezzati M, Kammen DM. Household energy, indoor air pollution and health in developing countries: Knowledge base for effective interventions. Annu Rev Energ Environ 2002;27:233-70.

Fullerton DG, and Bruce N. Indoor air pollution from biomass fuel smoke is a major health concern in the developing world. T Roy Soc Trop Med H 2008;102(9):843-51.

Edwards JHY, Langpap C. Fuel choice, indoor air pollution and children's health. Environ and Dev Econ 2012;17(4):379-406.

Pachauri S, Jiang L. The household energy transition in India and China. Energ Policy 2008;36(11):4022-35.

Ezzati M, Kammen DM. Household energy, indoor air pollution and health in developing countries: Knowledge base for effective interventions. Annu Rev Energ Environ 2002;27:233-70.

Bruce, N.; Perez-Padilla, R.; Albalak, R. Indoor air pollution in developing countries: A major environmental and public health challenge. Bull. World Health Organ. 2000, 78, 1078–1092.

WHO 2018 http://www.who.int/news-room/fact-sheets/detail/household-air-pollution-and-health

IHME. (2017). Global Burden of Disease Results Tool. Retrieved January 23, 2018, from http://ghdx.healthdata.org/gbd-results-tool

IIPS and ICF. (2017). National Family Health Survey (NFHS-4) 2015-16: India. Mumbai: IIPS: International Institute for Population Sciences and ICF.

IIT Bombay, HEI, IHME. (2018). Burden of Disease Attributable to Major Air Pollution Sources in Indi

Parikh, J. and Laxmi, V., Biofuels, Pollution and Health Linkages: A Survey of Rural Tamilnadu, Economic and Political Weekly, 2000.November 18-24, pp. 4125-4137.

Ministry of Non-conventional Energy Sources, 1997. National program on improved chulhas. Administrative approval 1997-1998, New Delhi, Government of India

Barnes, D. F., Kumar, P., Openshaw, K., 2012. Cleaner Hearths, Better Homes: New Stoves for India and the Developing, World, Oxford University Press, New Delhi, India.

Aggarwal, R.K. and Chandel S.S., Review of Improved Cookstoves Programme in Western Himalayan State of India, Biomass and Bioenergy, Volume 27, Issue 2, August 2004, pp. 131-144

Kishore, V.V.N., and Ramana, P.V., Improved cookstoves in rural India: how improved are they? A critique of the perceived benefits from the National Program on Improved Chulhas (NPIC), Energy, Volume 27, Issue 1, 2002,pp. 47-63

Ministry of New and Renewable Energy, 2010. New Initiative for Development and Deployment of Improved Cookstoves: Recommended Action Plan Final Report Prepared by Indian Institute of Technology Delhi and The Energy and Resources Institute, MNRE, New Delhi, Government of India

Smith, K. R., & Sagar, A. D. Making the clean available: Escaping India's Chulha Trap. 2014,Energy Policy, 410-414.

Prayas. (2018). Fuelling the transition: Costs and benefits of modern cooking fuels as a health intervention in India.

Desai, S., & Vanneman, R. India Human Development Survey -II (IHDS-II) 2011-12. Ann Arbor MI2016: ICPSR36151-v5

Parikh J, : Hardships and health impacts on women due to traditional cooking fuels: A case study of Himachal Pradesh, India Energy Policy 39 (2011) 7587–7594

Update, N. (2016, March 16). Cabinet approves Pradhan Mantri Ujjwala Yojana – Scheme for Providing Free LPG connections to Women from BPL Households . Retrieved from http://www.pmindia.gov.in/en/news_updates/cabinet-approves-pradhan-mantri-ujjwala-yojana-scheme-for-providing-free-lpg-connections-to-women-from-bpl-households

World Health Organizations, 2004. Indoor Air pollution, Household Energy and Millennium Development Goals

United Nations Development Programme, 2005. Energy Services for the Millennium Development Goals

Sesan, T.A., 2012. Navigating the limitations of energy poverty: Lessons from the promotion of improved cooking technologies in Kenya. Energy Policy, 47, 202–210

Jessica, J., Lewis, Bhojvaid, V., Brooks, N., Das, I., Jeuland, M. A., Patange, O., & Pattanayak, S. K., 2015. Piloting Improved Cookstoves in India, Journal of Health Communication: International Perspectives, 20: sup1, 28-42, DOI: 10.1080/10810730.2014.994243

Gupta S., Saksena S., Shankar R. & Joshi V. 1998, Emission factor and thermal efficiency of cooking biofuels from five countries. Biomass and bioenergy, 14(5-6), 547-559.

Joon, V., Chandra A., Bhattachrya M., 2009. Household energy consumption pattern and socio-cultural dimensions associated with it: A case study of rural Haryana, India, Biomass & Bioenergy, volume 33, issue 11, pp. 1509 – 1512

CRISIL. (2016). Assessment report: Primary survey on household cooking fuel usage and willingness to convert to LPG

FLDI. (2016, May 18). Letter from the Federation of LPG Distributors of India to Joint Secretary (M), MoPNG .

FLDI. (2016a, July 4). Letter from Federation of LPG Distributors of India to Joint Secretary (M), MoPNG.

International Journal of Advance and Innovative Research
Volume 8, Issue 4 (IV) October - December 2021
ISSN 2394 - 7780

PREPARATION AND STRCUTURAL STUDIES OF SOME BIS POLYMERIC COMPLEXES

Vaishali P. Meshram
Department of Chemistry, Dharampth M. P. Deo Memorial Science College, RTM Nagpur University, Nagpur, Maharashtra, India

ABSTRACT
Synthesis of inorganic polymer is an emerging field that covers a wide range of disciplines including the frontiers of chemistry, materials, medicine, electronics, optics sensors, information storage, energy conversion, environmental protection aerospace and many more. Chelate polymers have important applications in medical sciences like controlled drug delivery, artificial organs and protein synthesis. Some polymers can be made to be electrically conductive and offer potential for the semiconductor industry and as lightweight electrodes and electrolytes for batteries for automotive and aerospace applications. Newly developed polymers exhibit unusual optical properties that have attracted significant interest from the defense industries. Besides the synthesis of chelate polymers and examination of their thermal stability, present work describes structural characterization of these chelate polymers on the basis of elemental analyses infrared and reflectance spectra, magnetic and thermal studies. Since polymeric chelates are thermally resistant and have a large number of practical applications. Recently some chelate polymers have been synthesized, characterized and their thermal stability has been studied. Ligands of hydroxamic acid with adipic acid, azelaic acid, succinic acid, sebasic acid and subaric acid have been prepared in benzene medium by condensation process Now a day's proton NMR technique can be used for determination of stereochemical structure and conformational analysis of polymer compounds. The chemical shift in NMR spectrum, indicates that what type of hydrogen atoms are present e.g., methylene, methyl groups, olefins, ethers, esters and aromatic compounds. 2D-NMR methods have been used as a powerful and reliable techniques for determination of compositional and configurationally structure of co-ordination polymer. Polyvinyl pyridine and its copolymers have important applications as polyelectrolyte, polymer regents and in electrical applications. These ligands have been synthesized and characterized by various instrumental techniques.

Keywords –complexes, polymeric ligands, IR studies, spectral studies.

EXPERIMENTAL

Chemicals: All the chemicals used were AR grade (Merck). The solvents used were doubled distilled before used.

Instrumentions: ^{1}H-NMR ($CDCl_3$, DMSO-d_6) spectra were recorded on Bruker model DRX-30 NMR Spectrophotometer using TMS as internal reference (δ ppm)Carbon, Hydrogen and Nitrogen contents were analyzed on an EA 1108 Carlo Erba Elemental analyzer instrument at CDRI Lucknow. FTIR spectra were recorded on a Bruker IFS 66V Germany, spectrometer using the KBr technique at Regional Sophisticated Instrumentation Center, IIT Chennai. Reflectance spectra of the chelate polymers in solid state were recorded on a single beam Karl-Zeiss Jena, specord M-400 spectrophotometer, finely powdered barium sulphate was used as a reference material in the studies of reflectance spectra. Magnetic susceptibility of chelate polymers was determined by the Gouy's method at room temperature using mercury tetrathiocyanatocobaltate (II) as standard. The non-isothermal measurement of Mn (II), Co (II), Ni (II) and Zn (II) were carried out using a TGS-2 thermogravimetric analyzer along with a TADS computer system at the Regional Sophisticated Instrumental Center, Nagpur University, Nagpur. The thermocouple used was Pt-Pt-Rh with a temperature range of 20-1000^{0}C, 12mg sample was taken and the heating rate 15^{0}C/min was employed. The thermal analyses were carried out in air atmosphere and mass loss was recorded continuously on the recorder.

Preparation of dichloride of adipic, azelaic, succinic, sebasic and subaric acid: A quantity of (0.1m mol) dry acid and (0.25m mol) double distilled thionyl chloride was taken in 100ml dry round-bottomed flask fitted with water condenser provided with guard tube containing unhydrous calcium chloride. Flask was heated on a water bath for about 2-3 hours, till clear solution was obtained. The reaction mixture was then refluxed under reduced pressure for 30 min. to remove sulphur dioxide, hydrogen chloride and unreacted thionyl chloride.

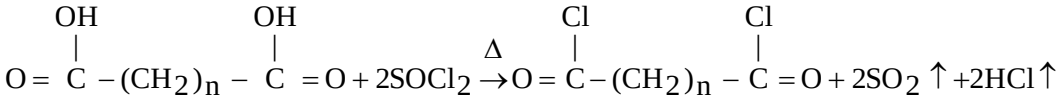

ISSN 2394 - 7780

(1) *n=4* for adipic acid (2) *n=7* for azelaic acid (3) *n=2* for succinic acid (4) *n=8* for sebasic acid (5) *n=6* for subaric acid.

Preparation of ligand: In present investigation, a modified method Priyadarshini and Tandon[6] based on Schotten Baumann reaction, was used for the preparation of hydroxamic acid. In this procedure hydroxylamine hydrochloride and vacuum distilled acid chloride in stoichiometric ratio were reacted at low temperature 0^0C or lower in diethylether medium containing aqueous suspension of sodium bicarbonate. Hydroxamic acid was prepared by the reaction of acid dichloride with excess of hydroxylamine hydrochloride in aqueous ethanol medium containing suspension of sodium bicarbonate, (0.25M) hydroxylamine hydrochloride A.R. grade, ethanol (50 ml) and sodium bicarbonate (0.5 M) and distilled water (25 ml) were placed in 500 ml beaker and acid dichloride was added (0.1 M) dissolved in 100 ml diethyl ether by dropping funnel during a period of 45 minutes with constant stirring. Mechanical stirrer was used for this. The stirring was further continued for 15 minutes. A granular solid mass was separated which was filtered and triturated with saturated solution of sodium bicarbonate in a porcelain mortar to remove any acidic impurities present and was then filtered and re-crystallized out in ethanol: DMF mixture. This ligand is reported first time in the present work and hence characterized by elemental and infrared spectral analyses[1-4]. The reaction of ligand formation has shown in Fig.1

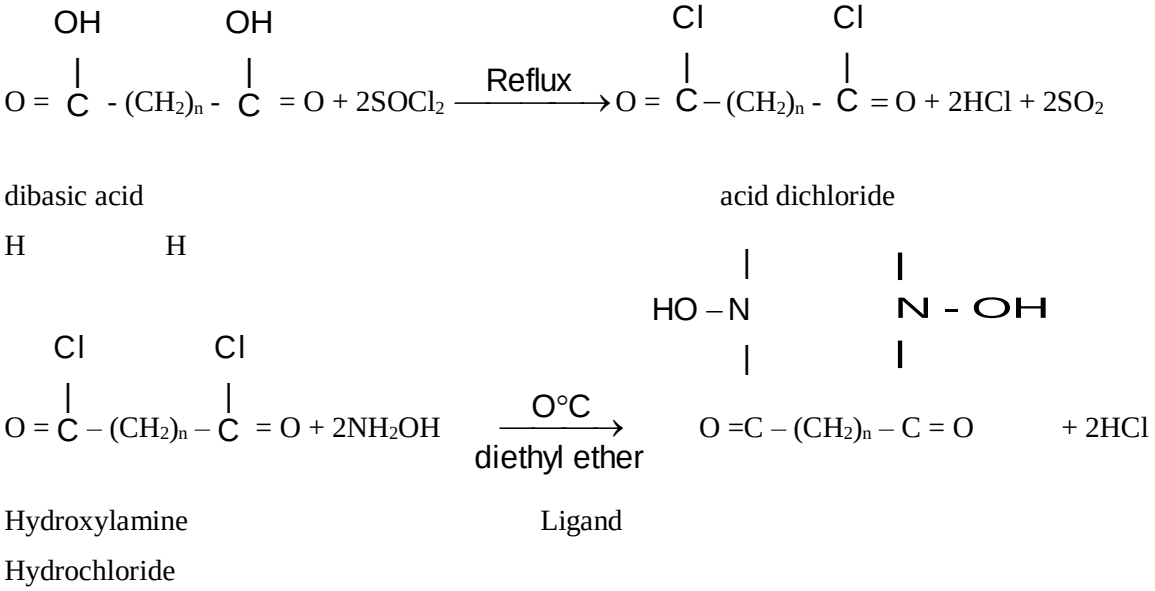

Fig. 1 - Synthesis of hydroxamic acid (ABHA)

Synthesis of chelate polymers of ligand

Chelate Polymers of with Mn (II), Co (II), Ni (II) and Zn (II) have been prepared by dissolving metal acetate (0.01M) separately in minimum amount of DMF and was added to a solution of hydroxamic acid (0.01 M) in (25 ml) DMF. The reaction mixtures were heated on an oil bath with constant stirring at 120 ^{0}C temperature. The chelate polymers generally appeared after 24-hrs heating on an oil bath. These chelate polymers obtained were filtered, washed thoroughly first with hot DMF and then with absolute alcohol and dried.

RESULTS AND DISCUSSION:

The ^{1}H-NMR Spectrum of hydroxamic acid ligands with adipic acid, azelaic acid, succinic acid, sebasic acid and subaric acid in acetone solvent along with complete assignments of resonances signals for aliphatic and aromatic protons are shown[5-6]. The NMR signal around δ(chemical shift) 2.05-2.40 ppm is assigned to the over laps of –CH2-protons of Ligands [7] . The aromatic protons of two phenyl groups are appeared at δ 7.48-7.63 ppm due to the presence of(-NHC=O) amide groups attached directly to benzene ring [8] and other resonance signal around δ 7.35-7.47 ppm is assigned due to two protons of benzene ring at which bromine attached[9-10] .

The resonance weak signal around δ 4.54-5.64 ppm is assigned to –NH-region of ligands and other weak signal around δ 8.24-8.27 ppm is assigned two protons of amide group (-NHC=O) [11] . In the infrared spectrum of the ligands a weak bands appeared from 3427-3480 cm^{-1} due to the presence of stretching vibration of the NH group [12]. Another sharp bands observed from 1606-1700 cm^{-1} may be assigned due to the C=0 stretching vibration[13] . A weak band appeared from 2882-2940 cm^{-1} may be assigned due to stretching vibrations of –CH_2– groups.

ISSN 2394 - 7780

Composition of the polymeric unit: the composition of the polymeric unit was assigned on the basis of detailed study of elemental analyses. The presence of water of crystallization was ascertained on the basis of thermal studies. The composition of polymeric unit is $[M(II)L]_n$, $\{[M'(II)(L)2H_2O]H_2O\}_n$ whereas (M= Zn(II), (M'= Mn(II), Ni (II) and Co(II)) (L = ABHA ligand).On the basis of elemental analyses, infrared spectra, reflectance spectra, magnetic measurements and thermal studies, the proposed structure of these chelate polymers .

Infrared spectral studies: In infrared spectra, a broad band appears at 3257 cm^{-1} in ABHA ligand may be assigned to the O-H stretching vibration [14]. A band appears at 1664 cm^{-1} in ABHA may be due to the resonating structure of the N-N-(C=O)-OH moiety. A band appears at 968 cm^{-1} may be assigned to the N-O stretching vibration.

The hydroxamic acids generally form five membered chelate ring with a metal ion and coordination takes place through >N-O and >C=O oxygen. As is anticipated, a band due to the O-H group disappears in polymers. Whereas a band due to the carbonyl group is shifted towards lower frequency side indicates that there is the formation of C=O → M coordinated bond. The N-O band in polymers found to have been shifted slightly to higher frequency side with increase in its intensity. A medium band appears in the region of lower frequency may be assigned to the M-O bonding in chelate polymers. Thus, from the above discussion and from the consideration of potential donor atoms of the polyligands, it can be concluded that the substituted-bis-hydroxamic acids act as bidentate ligands and participated in bonding through the phenolic oxygen and the oxygen of the C=O group to give neutral linear chain chelate polymers.

REFERENCES:

1. L.M.Jackman and S.Sternhell, Application of Nuclear Magnetic Resonance Spectroscopy in organic chemistry, 2nd Ed.(Oxford;Pergaman Press,1969).
2. J.S.Waugh, Analytical Chemistry, 65, no.17 (1993)725A-9A.
3. A.S.Brar and R.J.Kumar, Polym.Sci.Part A; Poly.chem. 84(2002)50.
4. A.S.Brar, Hooda S.and Kumar R., J.Polym.Sci. Part A; 84(2002)50.
5. Sunita Hooda, Rajeev Kumar and Manpreet Kumar, Indian J.of chemistry, 43 A (2004)527-531.
6. Vogels, Text book of Practical Organic Chemistry, Fifth Edition, Revised by Briam S. Furniss, Antoy J. Hannaford, Peter W. Smith and Austin R. Tatchell, 965.
7. R. J. Abraham, J.Fisher and P.Loftus, Introduction to NMR Spectroscopy (New York, Wiley, 1998).
8. Michael Mcgregor, NMR Spectroscopy, Hand book of instrumental Techniques for Analytical Chemistry, 316.
9. A. E. Tonelli, NMR Spectroscopy and Polymer Microstructure, The conformational connection (New York; VCH, 1989).
10. Laurent F.Groux,Thomas Weiss,Dastigin N.Reddy,Preston A.Chase,Warren E.Piers,Tom Ziegler,Masood Parvez and Jordi Benet-Buchhotz,J.AM.Chem.Soc.Vol.127,No.6(2005)1865.
11. Robert M.Silverstein, Francis X.Webster, Spectrometric Identification of Organic Compounds, John Wiley and Sons Inc.New York, 1998.
12. W. B. Gurnule, P.K.Rahangdale, L.J.Paliwal and K.B.Kharat, Reactive and Functional Polymers 55(2003)255-265.
13. Ashaq Hussain, Sheikh H. N.and Kalsotra B.L., J.Indian Chem. Soc., 83,531-535, (2006).
14. Azza A. A. Abu-Hussen, Journal of Coordination Chemistry, Vol. 59, No. 2, 157-176, (2006).

International e-Conference on New Horizons And Multidisciplinary Applications In Science And Technology
In Association withInternational Journal of Scientific Research in Science and Technology
Volume 9 | Issue 6 | Print ISSN: 2395-6011 | Online ISSN: 2395-602X (www.ijsrst.com)

Physico-Chemical Characterization of Mine Water Produced During Various Mining Activities, Treatment and Possible Usage

Vaishali P[1]. Meshram*[2], Pravin U. Meshram[1]

[1]Associate professor, Department of Chemistry, Dharampeth M. P. Deo Memorial Science College, Nagpur, Maharashtra, India

[2*]Associate Professor & Head, Department of Environmental Science, Sevadal Mahila Mahavidyalaya & Research Academy, Nagpur, Maharashtra, India

ABSTRACT

Investment plays a vital role in a developing country such as India, as it provides the necessary funds for undertaking productive activities to be circulated in the economy. Savings are our country's largest source of investment. Investments are assume they control their own destiny, whereas individuals with external LOC relate their experiences to destiny, luck or chance. Consequently, LOC has a great influence on an individual's investment decision-making behaviour. As a result, this study attempts to assess the LOC of an individual and segment the investors based on their level of internal and external LOC.

Keywords: Locus of control, Individual investor, Segmentation of investors.

I. INTRODUCTION

To estimate the Physico-chemical characterization of mine water produced during various mining activities, treatment and possible usage

II. OBJECTIVES

The mining industries are discharging millions of litres of water every day to the adjacent water courses creating water pollution problems in and around the mining area. Therefore it becomes essential to first assess the mine water quality and based on characteristics put it for beneficial usages (recycle and reuse), so as to avoid the mine water for its beneficiary use discharge pattern creating water pollution problems rather use it in the industry itself to save the fresh water requirement.

III. MATERIAL AND METHODS

i) **Sampling Site:** Mine water samples were collected phase wise (extractions) from ponds where the mine water was stored. Mine water samples were collected in polyethylene bottles of 1 litre capacity.

ii) **Analysis of mine water:** All the parameters reflecting mine water quality were analyzed as per the standard method (WHO standards).

IV. RESULTS AND DISCUSSION:

1. Mine water quality Assessment:

A classification of mine water is made based on the characteristics of mine waters from coal and non-coal mines i.e. alkaline mine water (A1, A2 and A3) and acidic mine water (B1 and B2). The characteristics of these mine waters are summarized in different categories as shown in **Table 1.**

The characteristics and the levels of concentration are shown in **Tables 2 to 5**. The characteristics of mine water collected from different mines are compared with water quality Standards (WHO, 2008 and IS 10500).

The results of analysis of collected mine waters in different seasons are depicted in **Tables 3, 4, and 5**. The pH of all mine water samples were found to be alkaline in nature, pH ranged from 7.2 to 8.2 with dissolved solids in the range of 83-301 mg/l, buffering capacity in the form of alkalinity ranged from 111-145 mg/l, turbidity in the range of 27-198 NTU with hardness in the range of 45-80 mg/l. Further, the organic content was also estimated in the mine water and expressed in terms of BOD and COD. The DO levels were also significant and recorded. The concentration level of demand parameters in the form of DO, BOD and COD ranged from 4.8-5.3 mg/l, < 3 mg/l and 6.8-11.3 mg/l respectively. It was observed that concentration levels of several metals like iron, zinc, chromium and cadmium ranged from 0.34 – 0.52 mg/l, 0.21-0.28 mg/l, 0.01-0.09 mg/l, and 0.2-0.3 mg/l respectively, whereas acidic mine water had pH in the range of 3.8-4.6, total dissolved solids 356-421 mg/l with hardness 78-102 mg/l. The demand parameters in the form of DO, BOD and COD ranged from 3.8-4.2 mg/l, ND and 30-56 mg/l respectively. From the characteristics of coal mine water, it was observed that the mine water was contributed by minerals with higher concentration levels of dissolved solids, however pH was found to be alkaline in nature. The organic load in terms of BOD was found to be less whereas COD was found to be in higher side might be due to the contamination of oil and grease and phenolic compounds.

This acidic mine water creates harmful effects on aquatic flora and fauna if discharged in water bodies and also to human beings if used for domestic purposes. Based on water quality characteristics, the acid mine water quality is categorized as B1 and B2 and shown in **Table 6**.

The overall characteristics of coal mine water was found to be alkaline in nature with permissible dissolved solids. However turbidity in the form of suspended load was found to be high dissolved oxygen was favorable to aquatic flora and fauna. Organic load observed was also not much and heavy metals content were in less concentration. Whereas the non-coal mine water quality was found to be acidic in nature, contains high dissolved solids due to the dissolution of minerals during mining process. The mine water was highly turbid in nature however levels of metal concentration were found to be low except iron content. It is mentioned that the alkaline mine water can be put in to use for domestic or irrigation purposes, whereas acidic mine water can-not be used for the same purposes unless treatment is given.

V. TREATMENT OF MINE WATER

Considering the mine water quality of both coal and non-coal mines, it becomes necessary to give treatment to the storage water in ponds or pits before put it into use. Alkaline mine water should be neutralized first and treated by applying coagulation and flocculation technique for the removal of suspended load or turbidity

followed by pressure filtration with disinfection treatment alongwith polishing with activated carbon. The acidic mine water, should be neutralized first with lime followed by sedimentation, filtration and polishing with activated carbon.

VI. RECYCLE AND REUSE

There is a plenty of scope for the application and reuse/recycle of mine water for the wastewater management in mining industry. The quality of the mine water whether it is alkaline or acidic should be neutralized and treated as mentioned above. The treated water further should stored in a mine out pits so that this will be the system of water harvesting and recharging of ground water also. This treated mine water could be used for water sprinkling for dust suppression during excavation and transportation activities. It could also be used for gardening depending on the soil quality and the characteristics of treated water to avoid any soil deterioration. Further, if the volume of mine water stored in mine out pits is in large quantity then, it is advisable to create a reservoir with plantation around for recreation and aesthetic point of view [17] (**Fig. 2-4**). This will provide a better and safer environment for future generation.

VII. CONCLUSION

Mine water sample were collected from coal and non-coal mine areas and analyzed with respect to quality parameters to assess the mine water quality. It was observed that there was variations in concentration levels of some quality parameters i.e. pH and total dissolved solids based on the composition of ores and mines. The mine water quality was compared with drinking water quality standards prescribed by WHO and CPCB. The mine water quality in both coal and non-coal areas was found to be much better, however, certain treatments for mine waters (both acid and alkaline) were suggested prior to put into use for domestic purposes.

Table 1: Characteristics of Alkaline Mine waters

	Unit	Category of the Alkaline Mine waters		
		A-1	A-2	A-3
Water Quality Parameters				
pH		7.7-8.5	7.0-8.5	6.0-8.0
Alkalinity	mg/l, as $CaCO_3$	200-7000	100-500	10-30
Hardness	mg/l, as $CaCO_3$	50-150	200-1500	1000
Total Dissolved Solids	mg/l	300-700	500-1500	1500-2500
ccTotal Suspended Solids	mg/l	5-30	12-50	10-50
Demand Parameters				
DO	mg/l	5.5-8.0	5.0-8.0	5.0-8.0
BOD	mg/l	<1	<1-2	<1-2
COD	mg/l	8-30	15-50	15-60
Element or Ion Content				
Calcium	mg/l, as Ca	10-50	50-200	100-150
Magnesium	mg/l, as Mg	10-30	40-180	80-100
Iron	mg/l	0-2	0-5	0-5

Sulphate	mg/l	10-100	100-800	1000 and above

Table 2: Characteristics of collected mine waters (post-monsoon) (Jharia coalfield)

Parameters	Unit	Phase I	Phase II
pH		7.2	8.27
EC	µS/cm	157	152
Turbidity	NTU	90	153
Total Dissolved Solids	mg/l	116	115
Total Alkalinity	mg/l as $CaCO_3$	128	133
Total Hardness	mg/l as $CaCO_3$	45	70
CO_3^{--}	mg/l	7.20	11.0
HCO_3^{-}	mg/l	180	210
Fe^{+3}	mg/l	0.60	0.40
Ca^{+2}	mg/l	30	40
Mg^{+2}	mg/l	15	30
Na^{+}	mg/l	7.7	5.40
K^{+}	mg/l	3.10	2.80
As^{---}	mg/l	0.01	0.01
SO_4^{--}	mg/l	1.33	1.70
PO_4^{---}	mg/l	1.20	1
SiO_2^{--}	mg/l	36	36
NO_3^{-}	mg/l	0.18	0.12
Cl^{-}	mg/l	5.32	5.96
NH_3	mg/l	ND	ND
DO	mg/l	5.10	4.80
BOD	mg/l	<3	<3
COD	mg/l	8.2	10.8
Cd^{+2}	mg/l	0.05	0.028
Zn^{+2}	mg/l	0.21	0.24
Cr^{+3}	mg/l	0.09	0.02

ND: Not detectable

Table 3: Characteristics of collected mine waters (water season)(Jharis coal field)

Parameters	Unit	Phase I	Phase II
pH		8.03	7.33
EC	µS/cm	91	174
Turbidity	NTU	28	34
Total Dissolved Solids	mg/l	83	127
Total Alkalinity	mg/l as $CaCO_3$	113	125

Total Hardness	mg/l as $CaCO_3$	80	71
CO_3^{--}	mg/l	9	6
HCO_3^{-}	mg/l	146	177
Fe^{+3}	mg/l	0.45	0.34
Ca^{+2}	mg/l	55	45
Mg^{+2}	mg/l	25	26
Na^{+}	mg/l	6.20	7.20
K^{+}	mg/l	2.80	3.30
As^{---}	mg/l	0.01	0.01
SO_4^{--}	mg/l	1.30	1.23
PO_4^{---}	mg/l	1.20	1.10
SiO_2^{--}	mg/l	35	35
NO_3^{-}	mg/l	0.13	0.17
Cl^{-}	mg/l	6.39	6.03
NH_3	mg/l	0.25	0.17
DO	mg/l	4.80	4.60
BOD	mg/l	<3	<3
COD	mg/l	6.80	8.50
Cd^{+2}	mg/l	0.030	0.03
Zn^{+2}	mg/l	0.26	0.24
Cr^{+3}	mg/l	0.01	0.02

Table 4: Characteristics of collected mine waters (summer season)(Jharia coalfield)

Parameters	**Unit**	**Phase I**	**Phase II**	**Phase III**
pH		7.75	7.63	7.71
EC	µS/cm	352	323	403
Turbidity	NTU	90	198	27
Total Dissolved Solids	mg/l	256	241	301
Total Alkalinity	mg/l as $CaCO_3$	134	111	145
Total Hardness	mg/l as $CaCO_3$	55	46	60
CO_3^{--}	mg/l	6	21	26
HCO_3^{-}	mg/l	136	225	254
Fe^{+3}	mg/l	0.52	0.47	0.39
Ca^{+2}	mg/l	35	29	38.5
Mg^{+2}	mg/l	20	17	21
Na^{+}	mg/l	4.10	3.50	5.50
K^{+}	mg/l	2.13	1.90	2.70
As^{---}	mg/l	0.01	0.01	0.01
SO_4^{--}	mg/l	1.40	1.50	1.31
PO_4^{---}	mg/l	1.50	1.40	1.54

SiO_2^{--}	mg/l	43	53	45
NO_3^-	mg/l	0.15	0.19	0.18
Cl^-	mg/l	5.04	5.68	5.54
NH_3	mg/l	0.13	0.18	0.14
DO	mg/l	5.30	4.80	5.10
BOD	mg/l	<3	<3	<3
COD	mg/l	10.80	11.30	8.60
Cd^{+2}	mg/l	0.024	0.035	0.032
Zn^{+2}	mg/l	0.27	0.28	0.23
Cr^{+3}	mg/l	0.017	0.016	0.014

Table 5: Characteristics of collected mine waters (non-coal mine, North-East)

Parameters	Unit	Post-monsoon	Winter	Summer
pH		3.8	4.1	4.6
EC	µS/cm	586	712	648
Turbidity	NTU	112	148	160
Total Dissolved Solids	mg/l	356	421	388
Total Acidity	mg/l as $CaCO_3$	48	62	56
Total Hardness	mg/l as $CaCO_3$	78	84	102
Ca^{+2}	mg/l	30.4	33.3	40.8
Mg^{+2}	mg/l	5.6	7.6	12.8
Na^+	mg/l	4.10	3.50	5.50
Fe^{+2}	mg/l	3.2	2.8	6.1
DO	mg/l	3.8	2.2	3.8
BOD	mg/l	-	-	-
COD	mg/l	30.8	48.2	56.7
Trace elements (Al, Cr, Zn, Pb, Cu, Cd, Ni, Co)	µg/l	Present in less quantity to non detectable levels		

Table 6: Characteristics of Acid Mine waters

	Unit	Category of the Acid Mine waters	
		B-1	B-2
Water Quality Parameters			
pH		5.0-7.0	2.0-4.5
Acidity	mg/l, as $CaCO_3$	25-150	100-250
Hardness	mg/l, as $CaCO_3$	200-500	500-3500
Total Dissolved Solids	mg/l	400-800	1000-4000
Demand Parameters			
DO	mg/l	5.5-8.5	3.8-7.5
BOD	mg/l	1-2	1-5

COD	mg/l	10-60	20-100
Metal concentration			
Calcium	mg/l	20-80	100-250
Magnesium	mg/l	10-70	50-100
Ferric Iron	mg/l	0-20	10-250
Ferrous Iron	mg/l	200-600 and above	100
Trace Elements Al, Cu, Zn, Mg, Ni, Pb, Cr, Sb, etc		Present in less quantities depending types of strata	

Fig. 1: Sampling location for mine water collection in coal field area

Fig. 2: Open Cast Mining (Coal)

Fig. 3: Mining activities in hilly area with storage of excavated materials

Fig. 4: Mining activities with storage of mine water in mine out pit with plantation around